



# Tombusviruses Target a Major Crossroad in the Endocytic and Recycling Pathways via Co-opting Rab7 Small GTPase

Zhike Feng,<sup>a</sup> Jun-ichi Inaba,<sup>a</sup> Peter D. Nagy<sup>a</sup>

<sup>a</sup>Department of Plant Pathology, University of Kentucky, Lexington, Kentucky, USA

**ABSTRACT** Positive-strand RNA viruses induce the biogenesis of unique membranous organelles called viral replication organelles (VROs), which perform virus replication in infected cells. Tombusviruses have been shown to rewire cellular trafficking and metabolic pathways, remodel host membranes, and recruit multiple host factors to support viral replication. In this work, we demonstrate that tomato bushy stunt virus (TBSV) and the closely related carnation Italian ringspot virus (CIRV) usurp Rab7 small GTPase to facilitate building VROs in the surrogate host yeast and in plants. Depletion of Rab7 small GTPase, which is needed for late endosome and retromer biogenesis, strongly inhibits TBSV and CIRV replication in yeast and *in planta*. The viral p33 replication protein interacts with Rab7 small GTPase, which results in the relocalization of Rab7 into the large VROs. Similar to the depletion of Rab7, the deletion of either *MON1* or *CCZ1* heterodimeric GEFs (guanine nucleotide exchange factors) of Rab7 inhibited TBSV RNA replication in yeast. This suggests that the activated Rab7 has proviral functions. We show that the proviral function of Rab7 is to facilitate the recruitment of the retromer complex and the endosomal sorting nexin-BAR proteins into VROs. We demonstrate that TBSV p33-driven retargeting of Rab7 into VROs results in the delivery of several retromer cargos with proviral functions. These proteins include lipid enzymes, such as Vps34 PI3K (phosphatidylinositol 3-kinase), PI4K $\alpha$ -like Stt4 phosphatidylinositol 4-kinase, and Psd2 phosphatidylserine decarboxylase. In summary, based on these and previous findings, we propose that subversion of Rab7 into VROs allows tombusviruses to reroute endocytic and recycling trafficking to support virus replication.

**IMPORTANCE** The replication of positive-strand RNA viruses depends on the biogenesis of viral replication organelles (VROs). However, the formation of membranous VROs is not well understood yet. Using tombusviruses and the model host yeast, we discovered that the endosomal Rab7 small GTPase is critical for the formation of VROs. Interaction between Rab7 and the TBSV p33 replication protein leads to the recruitment of Rab7 into VROs. TBSV-driven usurping of Rab7 has proviral functions through facilitating the delivery of the co-opted retromer complex, sorting nexin-BAR proteins, and lipid enzymes into VROs to create an optimal milieu for virus replication. These results open up the possibility that controlling cellular Rab7 activities in infected cells could be a target for new antiviral strategies.

**KEYWORDS** endosome, lipid enzymes, plant, replicase complex, replication, retromer, tombusvirus, virus-host interactions, vps34, yeast

Positive-strand RNA [(+)RNA] viruses co-opt cellular resources to produce viral progeny through a replication process on subcellular membranes. Virus-induced specialized structures are formed, which are called virus replication factories or viral replication organelles (VROs) (1–8). The VROs not only contain the viral proteins and viral RNAs but also sequester subverted host factors into a membranous environment. Importantly, an optimal protein and lipid composition of VROs is required for the assembly of numerous viral replicase complexes (VRCs), which produce the viral (+)RNA progeny. VROs have to

**Citation** Feng Z, Inaba J, Nagy PD. 2021. Tombusviruses target a major crossroad in the endocytic and recycling pathways via co-opting Rab7 small GTPase. *J Virol* 95:e01076-21. <https://doi.org/10.1128/JVI.01076-21>.

**Editor** Anne E. Simon, University of Maryland, College Park

**Copyright** © 2021 American Society for Microbiology. All Rights Reserved.

Address correspondence to Peter D. Nagy, [pdnagy2@uky.edu](mailto:pdnagy2@uky.edu).

**Received** 25 June 2021

**Accepted** 13 August 2021

**Accepted manuscript posted online** 18 August 2021

**Published** 13 October 2021

spatially and temporally organize the viral replication process. In addition, the VROs must protect the viral RNAs from cellular defense mechanisms as well (1, 3, 5, 9, 10).

In the last decade, major progress was made in our understanding of the virus-induced complex rearrangements of cellular membranes and alterations in metabolic processes using tomato bushy stunt virus (TBSV) (11–13). Notably, TBSV exploits co-opted protein chaperones, translation elongation factors, DEAD box helicases, glycolytic enzymes, the actin network, and cellular membrane remodeling ESCRT (endosomal sorting complex required for transport) machinery for replication (3, 12, 14–16). Similar to many other (+) RNA viruses, TBSV induces spherules, which are vesicle-like invaginations in subcellular membranes (11, 17–21).

Tombusviruses belong to the large flavivirus-like supergroup that includes important human, animal, and plant pathogens. The small single-component (+)RNA genome of TBSV codes for five proteins, and two of these are essential replication proteins. p92<sup>pol</sup> is the RNA-dependent RNA polymerase (RdRp) protein, and it is translated from the genomic RNA (gRNA) via readthrough of the translational stop codon of the smaller p33 open reading frame (ORF) (22). The p33 replication protein is multifunctional: p33 is the master regulator of VRO biogenesis, functions as an RNA chaperone, and selects the viral (+)RNA for replication (22–24). Notably, TBSV replication proteins are also functional in *in vitro* assays and when expressed in the yeast model host *Saccharomyces cerevisiae* (25–27).

VRO biogenesis involves peroxisomes for TBSV or mitochondria for the closely related carnation Italian ringspot virus (CIRV). These viruses also usurp subdomains of the endoplasmic reticulum (ER) network, Rab1-positive COPII vesicles, and Rab5-positive endosomes (11, 28–32). Notably, TBSV induces and stabilizes the formation of membrane contact sites (MCSs) between the ER and peroxisomes, which are used for sterol enrichment within VROs (17, 33). Altogether, major remodeling of membranes takes place within VROs, including membrane proliferation, new lipid synthesis, and the enrichment of lipids such as phosphatidylethanolamine (PE), sterols, PI(4)P, and PI(3)P phosphoinositides (19, 34–36).

Previous studies with tombusviruses (29, 34) demonstrated that several components of the endosome-mediated trafficking pathway are recruited into viral replication in host cells. In addition to the Rab5-positive early endosomal compartments, TBSV also co-opts Vps34 PI3K (phosphatidylinositol 3-kinase), endosomal sorting nexin-BAR proteins, the retromer complex, and retromer tubular transport carriers (34, 37, 38). These findings suggested that the endosomal trafficking compartment seems to be crucial for TBSV replication.

The endosomal network, which includes early, late, and recycling endosomes, is a collection of pleomorphic organelles. The endosomes either sort membrane-bound proteins and lipids for vacuolar/lysosomal degradation or recycle cargos to other organelles, such as the Golgi apparatus or the plasma membrane. The highly conserved Rab7 small GTPase plays multiple roles in endosomal trafficking, late endosome (LE) maturation, LE fusion with the vacuole/lysosome, and vacuole biogenesis (39). The Rab7-positive LE acts as a central hub in the endocytic pathway and functions as a sorting station. In addition, the retromer complex is recruited to the endosomes via the activated GTP-bound Rab7 (Ypt7 in yeast) small GTPase (40, 41). In addition, Rab7 GTPase is a major player in several degradation processes, including autophagy, mitophagy, and lipophagy (39, 42, 43). Together with the retromer, Rab7 also affects mTORC1 signaling (44). Rab7 is involved in interactions between the late endosome and the ER to facilitate lipid transfer (45). Rab7 regulates lipid droplet dynamics and mitochondrial fission (46, 47).

Because Rab7 small GTPase is a major regulator of the endosomal/vacuolar trafficking pathway (48), we targeted the putative role of the Rab7 small GTPase in TBSV replication in this work. We find that TBSV co-opts Rab7 small GTPase and its heterodimeric GEF (guanine nucleotide exchange factor) cofactors into VROs via interaction between the p33 replication protein and Rab7 in yeast and plant cells. Usurping Rab7 helps

TBSV to co-opt Rab7 effectors and Rab7-positive membranes into VROs. These results open up the possibility that controlling cellular Rab7 activities in infected cells could be a target for new antiviral strategies.

## RESULTS

**Rab7 small GTPase is required for tombusvirus replication.** Our previous finding that the host retromer complex and the retromer tubular transport carriers are hijacked by tombusviruses to deliver host lipid enzymes for making the tombusvirus VROs (37) has opened up the question of whether the regulatory Rab small GTPases are also involved in this process. Naturally, the retromer complex is recruited to the endosomes through the activated GTP-bound Rab7 (Ypt7 in yeast) small GTPase (40, 41, 49). In addition, we have previously identified a couple of Ypt7 effectors, including the Vps35 retromer component and the Vps41 subunit of the homotypic fusion and vacuole protein sorting (HOPS) tethering complex, which were required for TBSV replication in yeast (37, 50). Therefore, cellular Rab7 might be needed for TBSV replication by affecting retromer complex recruitment to endosomes or other processes. This was tested in haploid *ypt7Δ* yeast, which lacks Rab7 GTPase. Northern blotting demonstrated that TBSV replicon (rep) RNA replicated only at an ~25% level in the absence of Ypt7 protein (Fig. 1A). Interestingly, as previously observed with retromer knockout yeast mutants (37), the p33 replication protein level decreased in *ypt7Δ* yeast (Fig. 1A). Complementation with wild-type (WT) Ypt7p expressed from a plasmid in *ypt7Δ* yeast led to the recovery of TBSV repRNA replication and p33 accumulation to almost WT levels (Fig. 1A, lanes 10 to 12). The overexpression of Flag-Ypt7p in WT yeast did not result in increased TBSV repRNA accumulation (Fig. 1A). Altogether, the yeast-based experiments suggest a proviral role for the Rab7 small GTPase in TBSV replication in yeast.

Comparable experiments with CIRV, a closely related tombusvirus, which, unlike TBSV, associates with mitochondrial membranes for replication (51, 52), showed an ~5-fold reduction in *ypt7Δ* yeast (Fig. 1B). Notably, the accumulation of the p36 replication protein is decreased in *ypt7Δ* yeast (Fig. 1B). Deletion of *YPT7* in yeast did not result in changes in replication or replication protein expression of Flock House virus (FHV), an unrelated (+)RNA virus (Fig. 1C), suggesting that general cellular perturbations caused by the lack of Ypt7p are not the main reason for the observed reduction of tombusvirus replication in *ypt7Δ* yeast.

Similar to other Rab GTPase protein family members, Ypt7p (Rab7) GTPase activation depends on GEFs (guanine nucleotide exchange factors), which stimulate the exchange of bound GDP for GTP. The Ypt7p GEF consists of the heterodimeric complex of Mon1p and Ccz1p proteins in yeast (42) and GEF orthologs in plants (53). The deletion of either *MON1* or *CCZ1* inhibited TBSV repRNA replication by ~6-fold and reduced the accumulation of the p33 replication protein in yeast (Fig. 1D and E). The similar inhibitory effects of *YPT7* deletion and the absence of Ypt7p GEFs on TBSV replication indicate that the activated Rab7 GTPase is required for TBSV replication in yeast. Altogether, the Rab7 small GTPase and its GEFs seem to provide proviral functions for both the peroxisome-associated TBSV and the mitochondrion-associated CIRV.

We also knocked down *Nicotiana benthamiana* RabG3f, the homolog of *Arabidopsis* Rab7B (54) and yeast Ypt7, to validate the above-described yeast data. Silencing of RabG3f (Rab7) via the tobacco rattle virus (TRV)-mediated virus-induced gene silencing (VIGS) approach had no obvious phenotype in *N. benthamiana* (Fig. 2A). However, the accumulation of TBSV gRNA decreased by ~7-fold in leaves of RabG3f-silenced plants (Fig. 2A). Also, the typical necrotic symptoms caused by TBSV in young *N. benthamiana* leaves were ameliorated in RabG3f-silenced plants (Fig. 2A). Silencing of the Mon1 GEF of Rab7 resulted in reduced TBSV RNA accumulation by ~5-fold and only mild TBSV-induced symptoms in *N. benthamiana* leaves (Fig. 2B). Thus, similar to the yeast findings described above, the active RabG3f (Rab7) is a proviral host factor. We note, however, that plants have many Rab GTPases, and the knockdown of Mon1 might also affect the

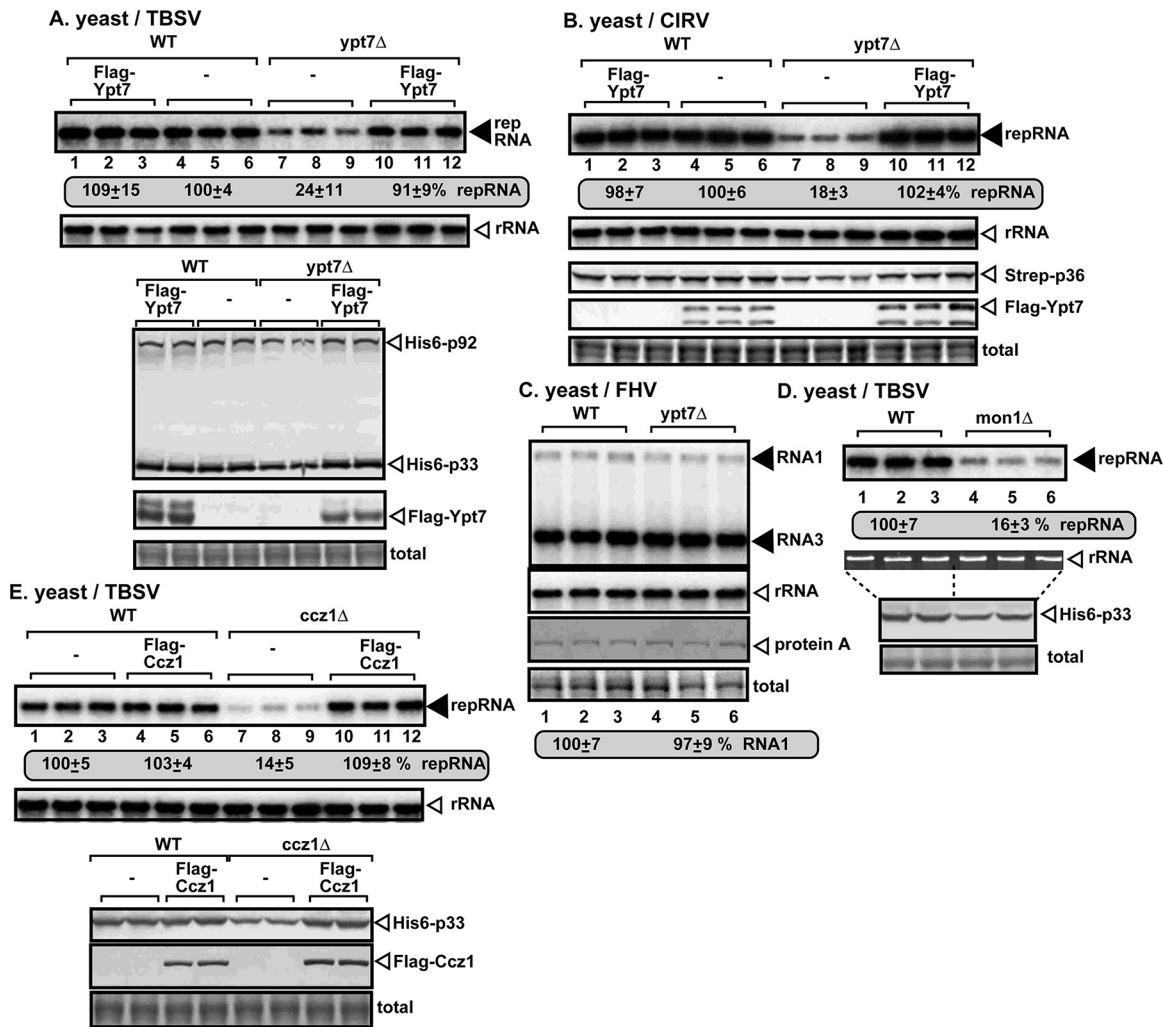


**FIG 1** Ypt7 small GTPase is an essential host factor for tomosvirus replication in yeast. Deletion of *YPT7* inhibits TBSV replication in yeast. (A, top) Northern blot analysis showing decreased TBSV (+)repRNA accumulation in the *ypt7Δ* versus WT yeast strains. Ypt7p was expressed from the *CUP1* promoter from a plasmid. Viral proteins His<sub>6</sub>-p33 and His<sub>6</sub>-p92 were expressed from plasmids under the galactose-inducible *GAL1* promoter, while DI-72 (+)repRNA was expressed from the *GAL10* promoter. The accumulation level of (+)repRNA was normalized based on 18S rRNA levels (second panel). (Bottom) The accumulation of His<sub>6</sub>-p33, His<sub>6</sub>-p92, and Flag-Ypt7 was measured by Western blotting with either anti-His or anti-Flag antibodies. Statistics were performed using an unpaired two-tailed *t* test, comparing the *ypt7Δ* strain to the WT for repRNA levels (*P* < 0.01). (B, top) Northern blot analysis showing reduced CIRV (+)repRNA accumulation in the *ypt7Δ* yeast strain. For further details, see the legend of panel A above. (Bottom) The accumulation of Strep-p36 and Flag-Ypt7 was measured by Western blotting with either anti-Strep or anti-Flag antibodies. Statistics were performed using an unpaired two-tailed *t* test, comparing the *ypt7Δ* strain to the WT for repRNA levels (*P* < 0.01). (C) Ypt7 small GTPase is not required for FHV replication in yeast. (Top) Northern blot analysis showing FHV RNA1 and subgenomic RNA3 accumulation in the WT and *ypt7Δ* yeast strains. (Bottom) The accumulation of HA-protein A was measured by Western blotting with anti-HA antibody. Statistics were performed using an unpaired two-tailed *t* test, comparing the *ypt7Δ* strain to the WT for FHV RNA1 levels (*P* > 0.05). (D, top) Northern blot analysis showing decreased TBSV (+)repRNA accumulation in the *mon1Δ* yeast strain. (Bottom) The accumulation of His<sub>6</sub>-p33 was measured by Western blotting and anti-His antibody. Statistics were performed using an unpaired two-tailed *t* test, comparing the *mon1Δ* strain to the WT for repRNA levels (*P* < 0.01). (E, top) Northern blot analysis showing decreased TBSV (+)repRNA accumulation in the *ccz1Δ* yeast strain. Ccz1p was expressed from the constitutive *TEF1* promoter from a plasmid. (Bottom) The accumulation of His<sub>6</sub>-p33 and Flag-Ccz1 was measured by Western blotting with anti-His or anti-Flag antibodies. Statistics were performed using an unpaired two-tailed *t* test, comparing the *ccz1Δ* strain to the WT for repRNA levels (*P* < 0.01). Each experiment was repeated twice.

function of other Rab GTPases, not solely RabG3f (55). Comparable experiments with the mitochondrion-associated CIRV showed an ~8-fold reduction in RabG3f (Rab7) knock-down *N. benthamiana* leaves (Fig. 2C).

Real-time quantitative PCR (RT-qPCR) analysis revealed an ~12-fold upregulation of the RabG3f mRNA level in the systemically infected leaves of *N. benthamiana* due to TBSV infection (Fig. 2D). This finding further supports the need for the usurped Rab7 to

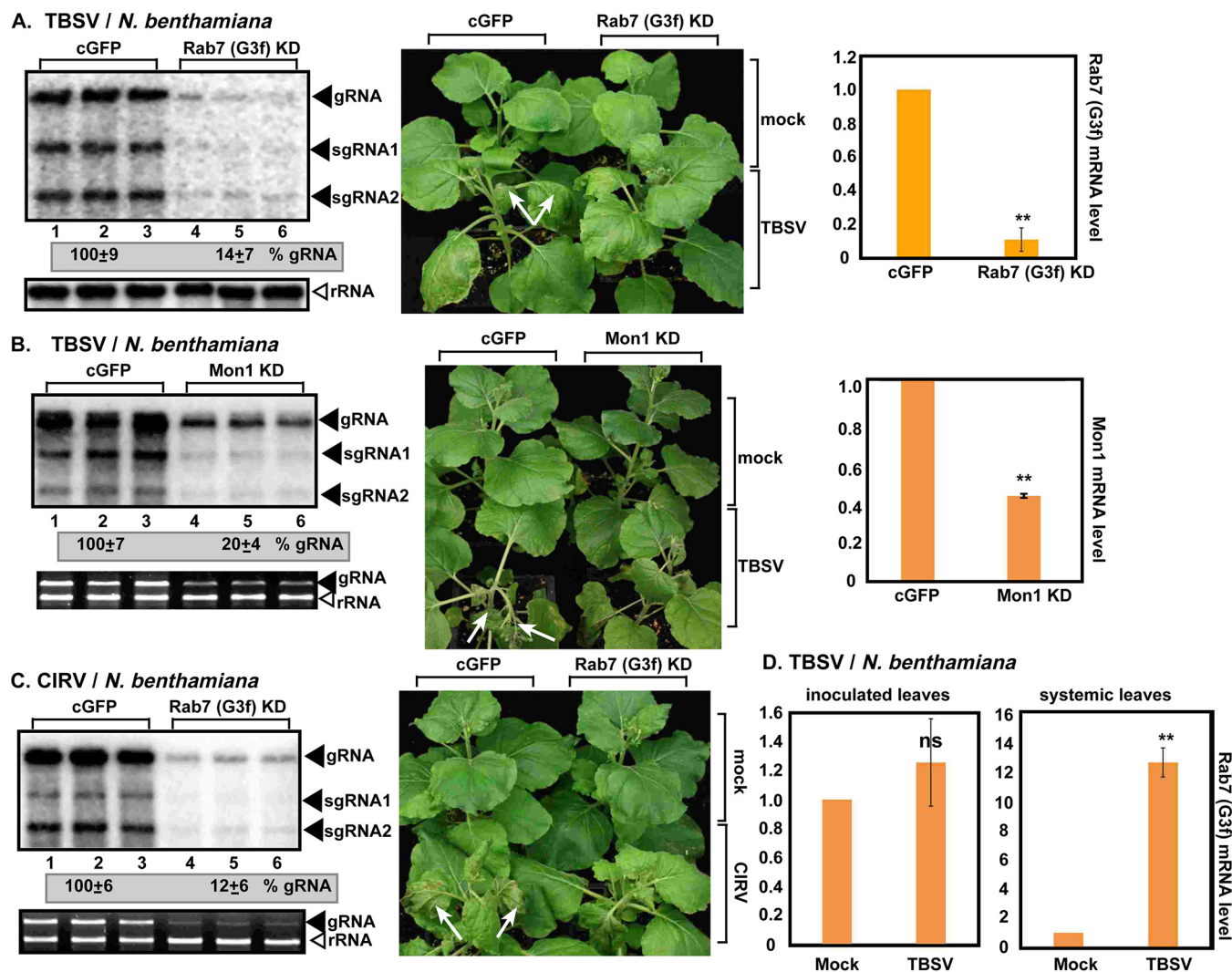


**FIG 2** Plant Rab7 small GTPase is required for tombusvirus replication. (A) VIGS-based knockdown (KD) of the NbRab7(G3f) mRNA level inhibits the accumulation of TBSV RNAs in *N. benthamiana*. (Top left) The accumulation of TBSV gRNA and subgenomic RNAs (sgRNAs) was measured using Northern blot analysis of total RNA samples obtained from *N. benthamiana* leaves at 2 dpi. The upper, systemically silenced leaves were inoculated with TBSV virions on the 12th day after VIGS. The control experiments included the TRV2-cGFP (C-terminal fragment of green fluorescent protein) vector. (Bottom left) Northern blot showing rRNA levels. (Middle) Delayed development of symptoms caused by TBSV infection in the Rab7(G3f)-silenced plants. (Right) Quantitative real-time PCR analyses of NbRab7(G3f) mRNA levels. Tubulin mRNA was used as an internal control in the VIGS plants. \*\*,  $P < 0.01$ . (B) VIGS-based knockdown of the NbMon1 mRNA level inhibits the accumulation of TBSV RNAs in *N. benthamiana*. (Top left) The accumulation of TBSV gRNA and sgRNAs was measured using Northern blot analysis of total RNA samples obtained from *N. benthamiana* leaves at 2 dpi. The upper, systemically silenced leaves were inoculated with TBSV virions on the 12th day after VIGS. (Bottom left) Ethidium bromide-stained gel showing rRNA levels. (Middle) Delayed development of symptoms caused by TBSV infection in the Mon1-silenced plants. (Right) Quantitative real-time PCR analyses of NbMon1 mRNA levels. Tubulin mRNA was used as an internal control in the VIGS plants. \*\*,  $P < 0.01$ . (C) VIGS-based knockdown of the NbRab7(G3f) mRNA level inhibits the accumulation of CIRV RNAs in *N. benthamiana*. (Left) The accumulation of CIRV gRNA and sgRNAs was measured using Northern blot analysis of total RNA samples obtained from *N. benthamiana* leaves at 2.5 dpi. For further details, see the legend of panel A above. (Second panel) Ethidium bromide-stained gel showing rRNA levels. (D) Quantitative RT-PCR analyses showing increased NbRab7(G3f) mRNA levels in inoculated leaves and leaves systemically infected with TBSV. \*\*,  $P < 0.01$ ; "ns," statistically not significant ( $P > 0.05$ ). Each experiment was repeated three times.

support intensive TBSV replication in plants. The putative effects of TBSV on other Rab7 family members in *N. benthamiana* will need future studies.

**Rab7 small GTPase is co-opted into VROs.** To gain insight into the role of Rab7 small GTPase in TBSV replication, we tested the localization of Ypt7p in yeast replicating TBSV. Confocal microscopy analysis revealed partial colocalization of red fluorescent protein (RFP)-Ypt7 with green fluorescent protein (GFP)-p33, which marks VROs in yeast (Fig. 3A). We also tested the localization of Rab7B in *N. benthamiana* plants infected with TBSV. Interestingly, RFP-tagged Rab7B from *Arabidopsis* is efficiently relocalized into the large VROs decorated with the blue fluorescent protein (BFP)-tagged

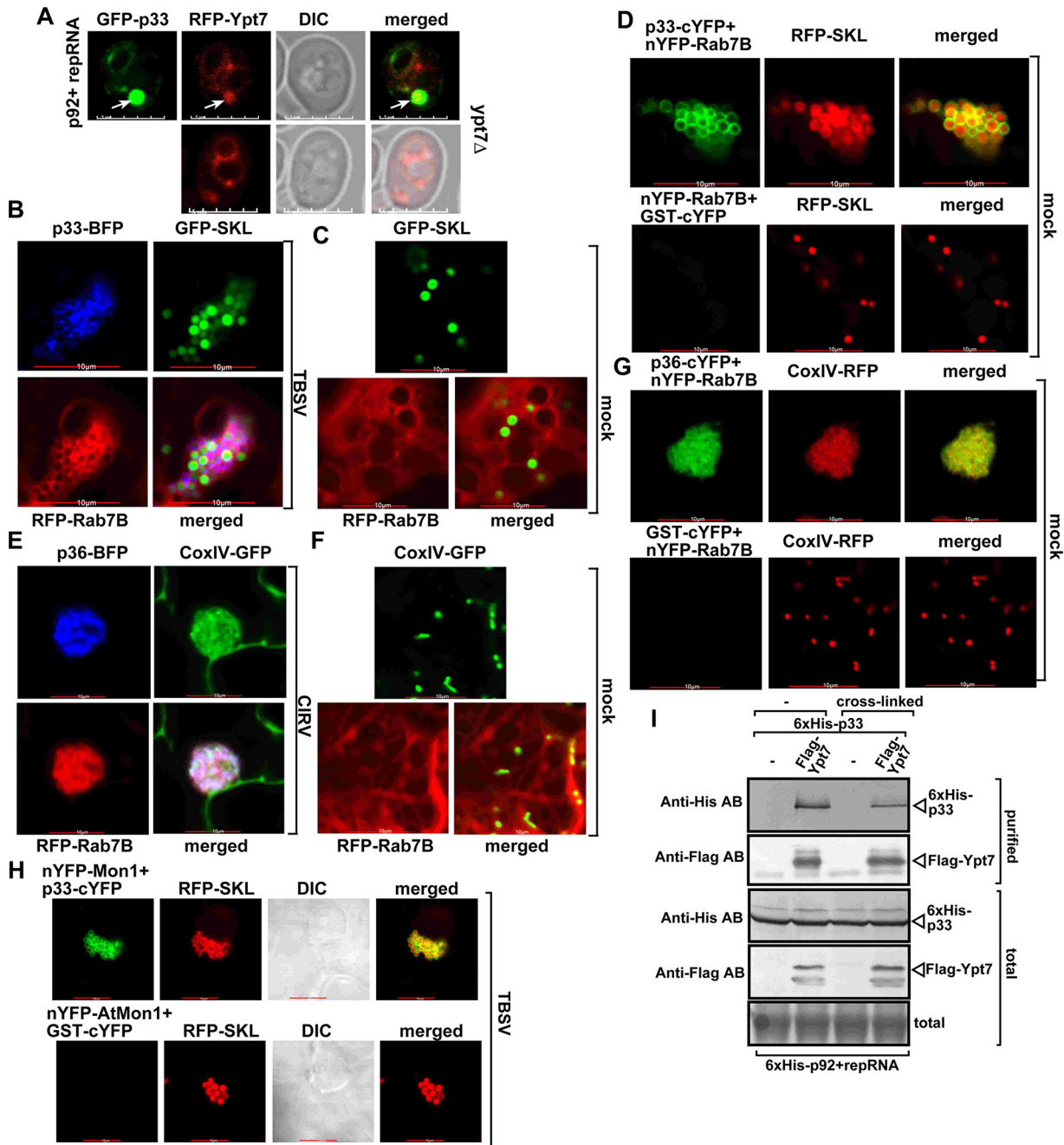


**FIG 3** Recruitment of Rab7 small GTPase by the tomosviral replication proteins into VROs. (A) Confocal laser microscopy images showing the partial colocalization of the TBSV GFP-tagged p33 replication protein with the RFP-tagged Ypt7p protein in *ypt7Δ* yeast cells replicating TBSV repRNA. The arrow points to the VRO in a yeast cell. Images on the bottom show the cellular distribution of Ypt7 in the absence of viral components. DIC, differential interference contrast. (B) Confocal microscopy images showing the colocalization of TBSV p33-BFP replication protein and RFP-AtRab7B in *N. benthamiana* plant cells. The large replication compartment was visualized via the expression of the GFP-SKL peroxisomal matrix marker protein. The expression of the above-described proteins from the 35S promoter was done after coagroinfiltration into *N. benthamiana* leaves. (C) Absence of colocalization of RFP-AtRab7B with GFP-SKL without viral components. For further details, see the legend of panel B above. (D) A BiFC assay was used to detect interactions between the p33 replication protein and the Rab7B protein *in planta*. TBSV p33-cYFP (C-terminal fragment of yellow fluorescent protein) or glutathione S-transferase (GST)-cYFP and nYFP (N-terminal fragment of YFP)-AtRab7B proteins were coexpressed from the 35S promoter after coagroinfiltration into *N. benthamiana* leaves. Note that the plants were not infected with TBSV. The colocalization of RFP-SKL (peroxisomal luminal marker) with the BiFC signal (see the merged image) demonstrates that the interaction between p33 and Rab7B proteins occurs in the VRO-like structures. (E) Confocal microscopy images showing the colocalization of CIRV p36-BFP replication protein and RFP-AtRab7B in plants. The large replication compartment was visualized via the expression of the CoxIV-RFP mitochondrial marker protein. (F) Absence of colocalization of RFP-AtRab7B with CoxIV-GFP without viral components. (G) A BiFC assay was used to detect the interaction between the CIRV p36 replication protein and the Rab7B protein *in planta*. CIRV p36-cYFP or GST-cYFP and nYFP-AtRab7B proteins were coexpressed from the 35S promoter after coagroinfiltration into *N. benthamiana* leaves. (H) A BiFC assay was used to detect the interaction between the p33 replication protein and the Mon1 protein *in planta*. TBSV

(Continued on next page)

p33 replication protein and the GFP-SKL peroxisome marker in *N. benthamiana* leaves (Fig. 3B). Rab7B was not associated with the peroxisomes, and it was more dispersed throughout the plant cells in the absence of TBSV replication (Fig. 3C). A bimolecular fluorescence complementation (BiFC) assay in *N. benthamiana* plants demonstrated that the interaction between Rab7B and the p33 replication protein occurred in VROs consisting of the aggregated peroxisomes (marked by the RFP-SKL peroxisomal marker) (Fig. 3D). Comparable experiments with CIRV also revealed the recruitment of Rab7B into VROs consisting of aggregated mitochondria in *N. benthamiana* (Fig. 3E and F). BiFC experiments further supported the relocalization of Rab7B into CIRV VROs and the interaction between Rab7B and the CIRV p36 replication protein in *N. benthamiana* (Fig. 3G). BiFC experiments also showed the relocalization of the Mon1 GEF of Rab7B into TBSV VROs and the interaction between Mon1 and the TBSV p33 replication protein in *N. benthamiana* (Fig. 3H).

TBSV replicase purification experiments from the detergent-solubilized membrane fraction of yeast showed the presence of copurified p33 and Ypt7p in Western blots (Fig. 3I). Altogether, these data firmly demonstrated that Rab7/Ypt7 is bound by the TBSV p33 and the CIRV p36 replication proteins, resulting in the recruitment of Rab7/Ypt7 into the VROs to support tombusvirus replication.

Rab7 requires PI(4)P-rich microdomains to initiate the recruitment of the retromer components to the endosomes (56). To sequester PI(4)P minor lipid species inside the yeast cells, we expressed the DrrA effector of *Legionella pneumophila*, which binds exceptionally strongly to PI(4)P (57). Accordingly, *Legionella* infection disrupts endocytic trafficking through inhibition of Rab7 and retromer functions in human cells (58, 59). The expression of the DrrA effector in leaves of *N. benthamiana* changed the localization pattern of Rab7B (Fig. 4A). Moreover, the p33-BFP replication protein did not colocalize with RFP-Rab7B (Fig. 4A), suggesting that TBSV failed to recruit Rab7-positive endosomal compartments to the site of replication in the presence of the DrrA effector. This is in contrast to the efficient recruitment of Rab7B into the p33-positive VROs in TBSV-infected leaves of *N. benthamiana* (Fig. 3B and Fig. 4B). These data indicate that TBSV targets Rab7 in specific PI(4)P-rich microdomains in the endosomes to hijack Rab7 and downstream effectors, as shown below.

**Rab7 small GTPase is needed for TBSV to hijack the retromer and the endosomal sorting nexin-BAR proteins into VROs.** The retromer complex and the retromer tubular carriers are hijacked by tombusviruses to deliver critical proviral host proteins, including the positive membrane curvature-sensing endosomal sorting nexin-BAR proteins and lipid enzymes, into VROs (37). The formation of the retromer complex depends on Rab7 (48, 54); therefore, we have tested if Rab7 is involved in co-opting the retromer into VROs. Coexpression experiments in *N. benthamiana* plants revealed that the retromer components Vps35, Vps26, and Vps29 and Rab7B GTPase were co-opted simultaneously into the tombusvirus VROs (Fig. 5A). In the absence of TBSV infection, the coexpression of RFP-Rab7B and the individual retromer components revealed partial colocalization in *N. benthamiana* plants, but these proteins were not part of large aggregates, unlike in TBSV-infected plant cells (Fig. 5B). The proposed proviral role of Rab7 in the subversion of the retromer complex by TBSV was tested via conducting BiFC experiments in *N. benthamiana* plants. The Vps29 retromer complex protein did not detectably interact with the p33 replication protein within VROs when RabG3f (Rab7) was knocked down by VIGS in *N. benthamiana* (Fig. 5C). As documented previously (37), Vps29 interacted with p33 and relocalized into VROs in control *N. benthamiana* plants (Fig. 5C).

### FIG 3 Legend (Continued)

p33-cYFP or GST-cYFP and nYFP-AtMon1 proteins were coexpressed after coagroinfiltration into *N. benthamiana* leaves. Note that the plants were infected with TBSV. (I) Copurification of yeast Ypt7p with the TBSV VRCs. (Top) Western blot analysis of copurified His-tagged p33 with Flag affinity-purified Ypt7 from the membrane fraction of yeasts replicating TBSV repRNA. The negative control was purified from yeast extracts using a Flag affinity column (lanes 1 and 3). The yeast samples were either cross-linked with formaldehyde or not cross-linked. (Second panel) Western blotting of purified Flag-Ypt7 detected with anti-Flag antibody (AB). (Bottom panels) Western blotting of Flag-Ypt7 and His<sub>6</sub>-p33 proteins in the total yeast extracts using anti-Flag and anti-His antibodies, respectively. Each experiment was repeated three times.

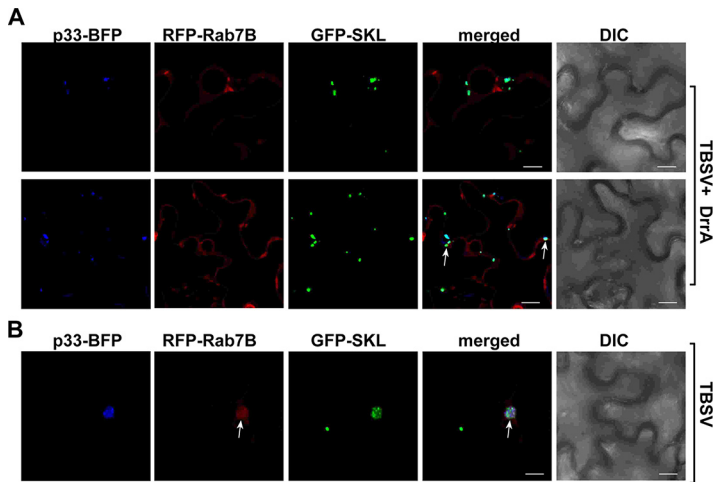


**FIG 4** Expression of the *Legionella* DrrA effector inhibits the recruitment of Rab7 into VROs in plants. (A) Coexpression of the *Legionella* DrrA effector with RFP-Rab7B, p33-BFP, and GFP-SKL was done after agroinfiltration in *N. benthamiana* leaves, which were inoculated with TBSV sap 1.5 days later. Confocal images were taken 2.5 days after agroinfiltration. Arrows point to p33-positive VROs in cells. Bars, 10  $\mu$ m. (B) Control experiments were performed in the same manner except omitting DrrA effector expression. Bars, 10  $\mu$ m. Each experiment was performed twice.

The endosomal sorting nexin-BAR proteins, namely, Vps5p in yeast and the orthologous Snx1 and Snx2a/b in plants, are recruited into TBSV VROs (38). Rab7 might assist p33 replication protein to subvert these sorting nexins. Accordingly, the recruitment of Vps5p sorting nexin into VROs was inefficient in *ypt7* $\Delta$  yeast, in contrast to the efficient

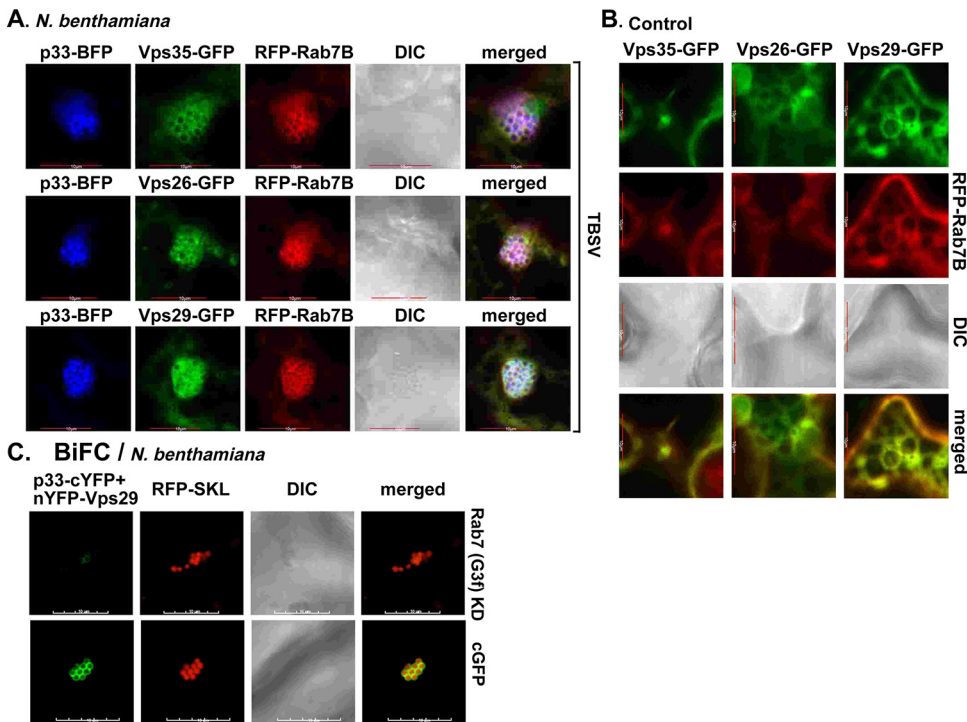


**FIG 5** Rab7 small GTPase is needed for TBSV to hijack the retromer proteins into VROs. (A) Colocalization of p33-BFP and RFP-AtRab7B with Vps35-GFP, Vps26-GFP, and Vps29-GFP retromer complex proteins within VROs in *N. benthamiana* leaves infected with TBSV. (B) Colocalization of Rab7B with the retromer proteins in the absence of TBSV infection. For further details, see the legend of panel A above. (C) BiFC assay showing reduced levels of interaction between TBSV p33 and Vps29 retromer protein in NbRab7(G3f)-silenced *N. benthamiana* leaves. RFP-SKL was expressed as a peroxisomal marker to identify VROs. Note that the plants were infected with TBSV. Each experiment was repeated three times.

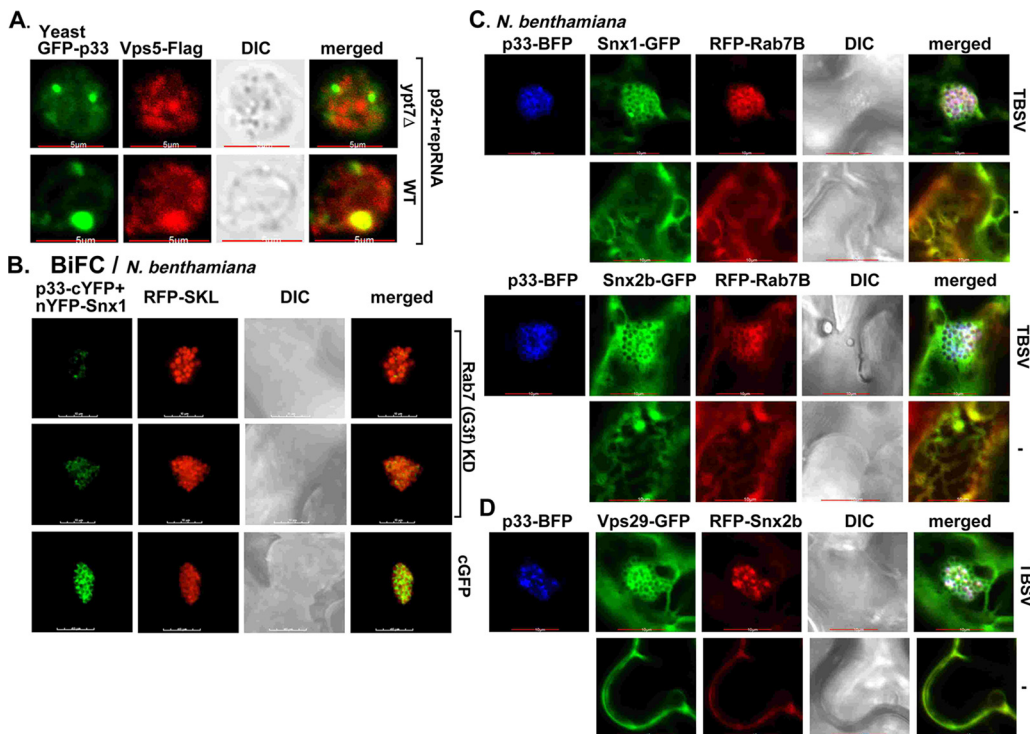


**FIG 6** Rab7 small GTPase is required for TBSV to co-opt the endosomal sorting nexin-BAR proteins into VROs. (A) Confocal laser microscopy images showing the lack of colocalization of Vps5 sorting nexin protein with TBSV p33 replication proteins in *ypt7Δ* yeast. Partial colocalization of Vps5 with the TBSV p33 replication proteins was observed in WT yeast. Note that yeasts also expressed p92<sup>pol</sup> and the TBSV repRNA. (B) BiFC assay showing decreased levels of interaction between p33 and Snx1 sorting nexin-BAR protein in *NbRab7(G3f)*-silenced *N. benthamiana* leaves. TBSV p33-cYFP and nYFP-Snx1 proteins were coexpressed after coagroinfiltration into *N. benthamiana* leaves. RFP-SKL was expressed as a peroxisomal marker to identify VROs. Note that the plants were infected with TBSV. (C) Colocalization of p33-BFP and RFP-AtRab7B with GFP-tagged Snx1 and Snx2b within VROs in *N. benthamiana* leaves infected with TBSV. (D) Colocalization of p33-BFP and RFP-Snx2b with Vps29-GFP within VROs in *N. benthamiana* leaves infected with TBSV.

relocalization of Vps5p into VROs in WT yeast (Fig. 6A). To test if Rab7 performs similar functions in plants, we silenced the RabG3f (Rab7) level, which dramatically reduced the BiFC signal between the Snx1 sorting nexin and the p33 replication protein compared with the BiFC signal detected in control *N. benthamiana* plants (Fig. 6B). Furthermore, the endosomal Snx1 and Snx2b sorting nexins were relocalized with RFP-Rab7B and p33 replication protein into VROs (Fig. 6C). Most of the Snx1 and Snx2a/b proteins are likely transported to VROs via the hijacked retromer tubular transport carriers (38). Indeed, we observed the colocalization of the Vps29 retromer component and Snx2b in the TBSV-induced VROs in *N. benthamiana* cells (Fig. 6D). Thus, Rab7/Ypt7p is involved in the recruitment of both the retromer complex and the sorting nexin-BAR proteins into TBSV VROs.

**The retromer does not deliver co-opted lipid enzymes into VROs when Rab7 is depleted.** The retromer tubular carriers are hijacked by tombusviruses to deliver critical lipid enzymes into VROs to modify the co-opted membranes' lipid composition (37). To further demonstrate the functional significance of Rab7 during TBSV replication, we tested if cellular lipid enzymes were co-opted into VROs when Rab7 was depleted. We have previously shown that TBSV co-opts the cellular lipid kinase Vps34 PI3K (phosphatidylinositol 3-kinase) (34). The subverted Vps34 then produces PI(3)P phosphoinositide from PI phospholipid, resulting in PI(3)P enrichment within VROs for optimal TBSV replication (34). PI(3)P phosphoinositide is bound by the co-opted sorting nexin-BAR proteins, which is critical for VRC structure/stability and protection of the viral RNA from host RNases (25, 38). We have deleted the *YPT7* gene from a yeast strain in which Vps34p was tagged with a 3×HA (hemagglutinin) tag in its original chromosomal location. After the expression of Flag-p33, Flag-p92<sup>pol</sup>, and the TBSV repRNA in yeast, Flag-p33 and Flag-p92<sup>pol</sup> were affinity purified

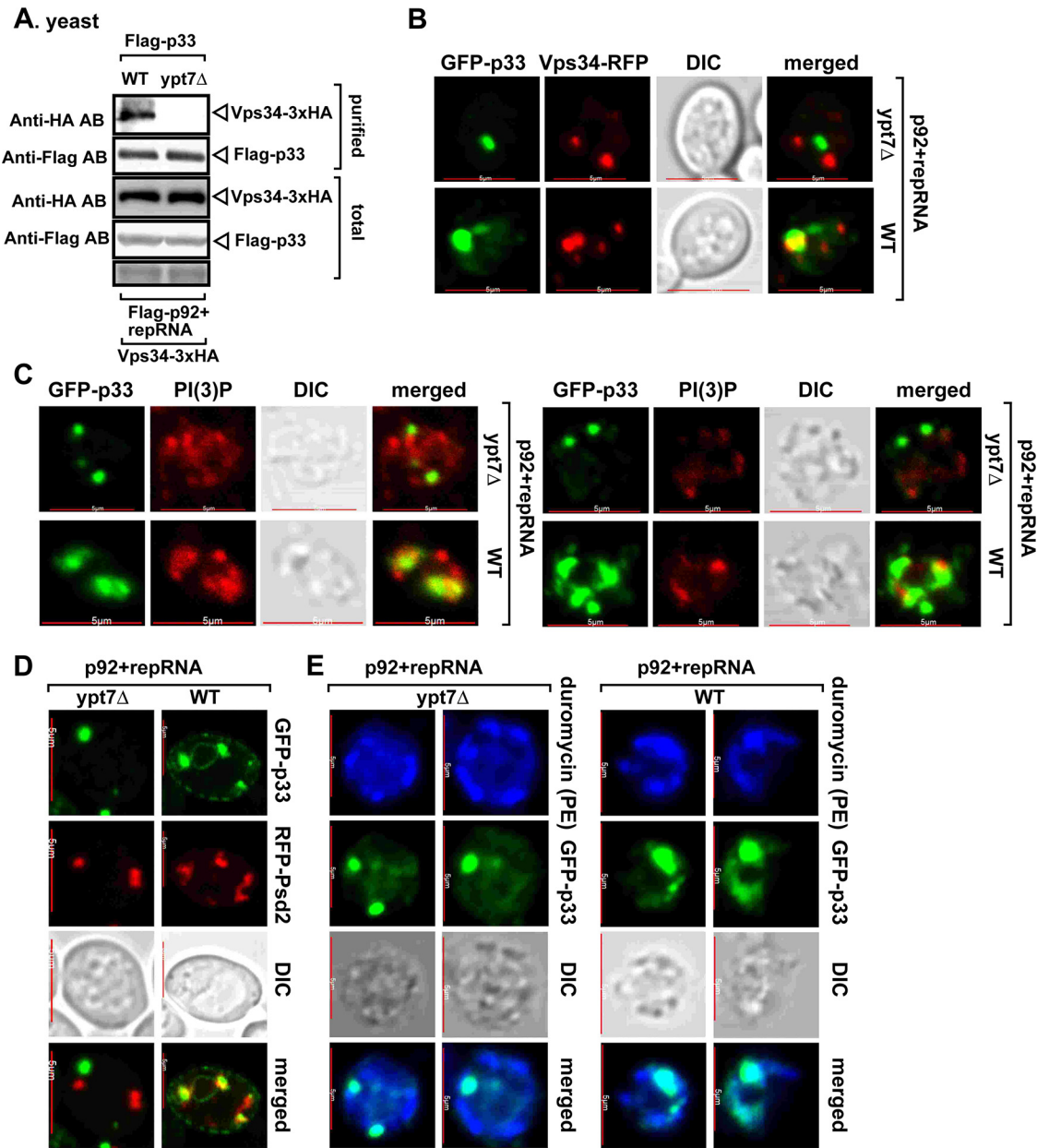


**FIG 7** Co-opted Rab7 small GTPase is needed to deliver Vps34 phosphatidylinositol 3-kinase and Psd2 phosphatidylserine decarboxylase into VROs. (A) Reduced level of copurified Vps34p with Flag affinity-purified TBSV p33 from subcellular membranes of the ypt7Δ yeast strain replicating TBSV repRNA. The top two panels show copurified Vps34-3×HA with the viral replicase using Flag-based purification from the detergent-solubilized membrane fraction. The bottom panels show Western blot analysis of Vps34-3×HA and Flag-p33 in the total yeast lysates with anti-HA and anti-Flag antibodies, respectively. (B) Confocal laser microscopy images showing the lack of colocalization of TBSV GFP-p33 replication protein with the Vps34-RFP protein in ypt7Δ yeast cells versus their colocalization in WT yeast cells. (C) Confocal laser microscopy images showing the lack of enrichment of PI(3)P phosphoinositide within VROs in ypt7Δ yeast cells versus their partial colocalization in WT yeast cells. The PI(3)P distribution was visualized via PI(3)P-specific antibody. Two sets of images are shown to document reproducibility. (D) Confocal laser microscopy images showing the lack of colocalization of TBSV GFP-p33 replication protein with the RFP-Psd2 protein in ypt7Δ yeast cells versus their colocalization in WT yeast cells. (E) Confocal laser microscopy images showing the lack of enrichment of PE phospholipid within VROs in ypt7Δ yeast cells versus their colocalization in WT yeast cells. The PE distribution was determined by using biotinylated duramycin peptide and streptavidin conjugated with Alexa Fluor 405. Each experiment was repeated three times.

from the detergent-solubilized membrane fraction, followed by Western blot analysis. We found that the absence of Ypt7p in this yeast strain led to a reduced amount of copurified Vps34p in the viral replicase preparation, in comparison with the control yeast (Fig. 7A). This finding suggests that Ypt7p (Rab7) is essential for the targeting of Vps34 PI3K to

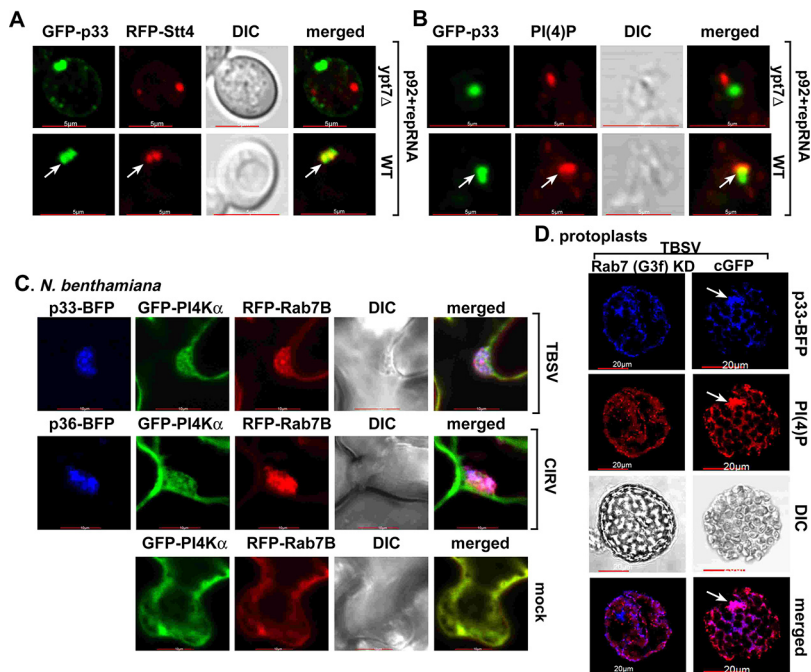


**FIG 8** Co-opted Rab7 small GTPase is needed to transport phosphatidylinositol 4-kinase (PI4K $\alpha$ -like) into VROs. (A) Confocal laser microscopy images showing the absence of colocalization of the TBSV GFP-p33 replication protein with the yeast PI4K $\alpha$ -like RFP-Stt4 protein in *ypt7Δ* yeast cells versus their colocalization in WT yeast cells. (B) Confocal laser microscopy images showing the lack of enrichment of PI(4)P within VROs in *ypt7Δ* yeast cells versus their colocalization in WT yeast cells. The PI(4)P distribution was visualized via PI(4)P-specific antibody in fixed cells. (C) Colocalization of RFP-AtRab7B with GFP-PI4K $\alpha$  within VROs in *N. benthamiana* leaves infected with either TBSV or CIRV. (D) Confocal laser microscopy images showing the lack of enrichment of PI(4)P phosphoinositide within VROs in NbRab7(G3f)-silenced plant leaves. The PI(4)P distribution was visualized via PI(4)P-specific antibody. Each experiment was repeated three times.

VROs. This conclusion was further supported by the lack of colocalization of GFP-p33 and Vps34-RFP in *ypt7Δ* yeast (Fig. 7B). Accordingly, we also noted the lack of enrichment of the critical PI(3)P phosphoinositide within VROs in *ypt7Δ* yeast (Fig. 7C). Rab7 is known to stimulate the lipid kinase activity of Vps34 to produce PI(3)P-rich microdomains.

Another co-opted lipid enzyme is Psd2 phosphatidylserine decarboxylase, which produces phosphatidylethanolamine (PE) within VROs (37). PE is a critical phospholipid for proper VRC functions during viral RNA synthesis (19, 25, 60). The deletion of *YPT7* inhibited the relocalization of Psd2p into VROs (Fig. 7D) and reduced PE enrichment within VROs in yeast (Fig. 7E).

We also tested the subversion of PI4K $\alpha$ -like Stt4 phosphatidylinositol 4-kinase, which produces PI(4)P phosphoinositide within VROs (37, 61). PI(4)P phosphoinositide has a crucial function in sterol enrichment within VROs, needed for protecting viral RNAs from host RNases (25, 61). The deletion of *YPT7* interfered with the targeting of Stt4p into VROs (Fig. 8A) and inhibited PI(4)P enrichment within VROs in yeast (Fig. 8B). PI4K $\alpha$  and Rab7B are colocalized with either TBSV or CIRV replication proteins within VROs in *N. benthamiana* plants (Fig. 8C). In addition, silencing of RabG3f (Rab7) resulted in reduced PI(4)P enrichment within the p33-positive VROs in *N. benthamiana* protoplasts compared with the PI(4)P distribution in the control protoplasts (Fig. 8D). Altogether, the yeast- and plant-based experiments showed that Rab7/Ypt7p is required for the subversion of proviral host lipid enzymes and the enrichment of phosphoinositides and PE phospholipid within tombusvirus VROs.

**The Rab7 small GTPase is not required for subversion of Rab5-positive early endosomes into VROs.** Tombusviruses subvert the Rab5-positive early endosomes into VROs to increase lipids and membrane surfaces that support viral replication. This is achieved via binding of the small p33/p36 replication protein to Rab5 small GTPase

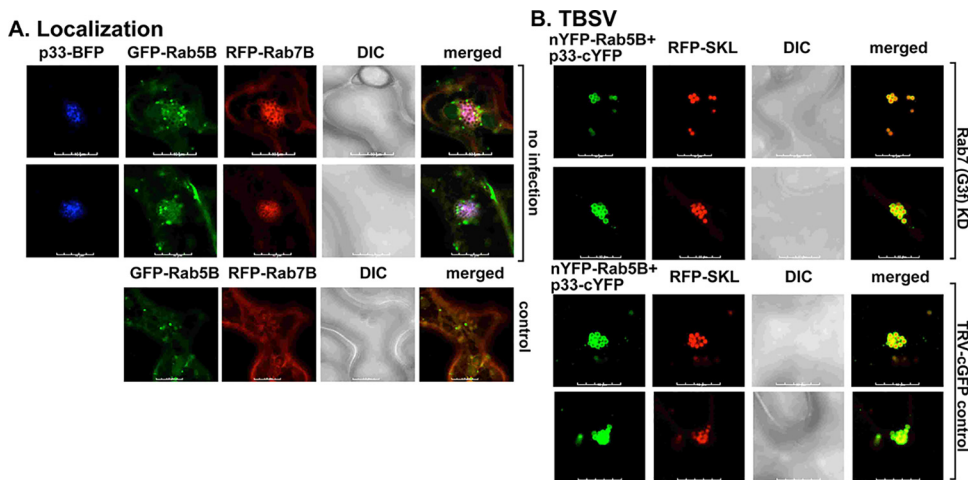


**FIG 9** Subversion of Rab5-positive early endosomes into VROs is not dependent on Rab7 small GTPase. (A) Colocalization of RFP-AtRab7B with GFP-AtRab5B within VROs labeled with p33-BFP in *N. benthamiana* leaves. (B) BiFC assay showing similar intensities of the interaction between p33 and Rab5B small GTPase protein in NbRab7(G3f)-silenced *N. benthamiana* leaves and TRV2-cGFP control leaves. TBSV p33-cYFP and nYFP-AtRab5B proteins were coexpressed after coagroinfiltration into *N. benthamiana* leaves. RFP-SKL was expressed as a peroxisomal marker to identify VROs. Note that the plants were infected with TBSV. Each experiment was repeated three times.

(29). Indeed, we found that GFP-Rab5B and RFP-Rab7B are relocalized to the p33-decorated VROs in *N. benthamiana* plants (Fig. 9A).

Knockdown of the RabG3f (Rab7) level in *N. benthamiana* plants did not visibly inhibit the interaction between the p33 replication protein and Rab5B, based on BiFC (Fig. 9B). The recruitment of Rab5B via the p33 replication protein in plants with RabG3f (Rab7) depleted suggests that TBSV can hijack the Rab5-decorated early endosomes independently of Rab7. However, we observed smaller VROs frequently in Rab7 knockdown plants compared with the control plants (Fig. 7B). These data suggest that Rab5 and Rab7 small GTPases do not play complementary roles in TBSV replication.

## DISCUSSION

The replication of (+)RNA viruses requires the subversion of intracellular organelles and vesicles that form VROs inside the cytosol of the infected cells (5, 6, 10, 13, 62–66). The extensive membrane surfaces within the VROs serve as a protective barrier against the host antiviral surveillance system (5, 9) and concentrate the viral RNA and the replication machinery (1, 67–73).

TBSV VROs consist of aggregated peroxisomes and associated subdomains of the ER membranes (17, 28, 30). TBSV has been shown to target the endosomal network to enhance membrane surfaces and modify the lipid composition of VROs (19, 29, 34). However, not all critical host factors usurped by TBSV are known yet. In the current study, we show evidence that TBSV targets Rab7 small GTPase, which functions at important crossroads of cellular trafficking. The interaction between the TBSV p33 replication protein and Rab7 leads to the recruitment of Rab7 into VROs. Although the hijacking of Rab7 by TBSV would likely affect the roles of Rab7 in late endosome/vacuolar trafficking or the autophagy process, in this paper, we demonstrate the critical role of the subverted Rab7 in the biogenesis of tombusvirus VROs. We find that TBSV exploits Rab7 function connected with the retromer complex, the retromer tubular transport carriers, and the endosomal sorting nexin-BAR proteins, which are efficiently recruited into VROs. The depletion of Rab7 in yeast or plants inhibited the replication of TBSV and the closely related CIRV by reducing the delivery of lipid enzymes, such as Vps34 PI3K, Psd2, and Stt4 PI4K, into VROs. We have shown previously that the lipid products of these co-opted enzymes are required for making up the optimal microenvironment

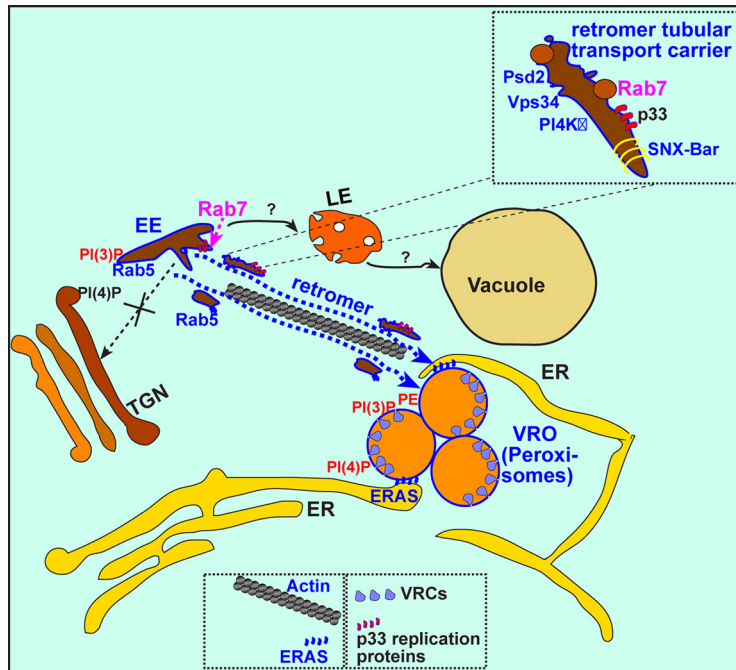


**FIG 10** Proposed role of Rab7 small GTPase in facilitating the delivery of Psd2 phosphatidylserine decarboxylase, Vps34 PI3K, PI4K $\alpha$ -like Stt4, and the endosomal sorting nexin-BAR proteins into TBSV VROs via retromer tubular transport carriers for tombusvirus replication. Note that CIRV uses a similar strategy for the recruitment of the above-mentioned host proteins into VROs formed from the aggregated mitochondria. Question marks indicate the possible but not yet demonstrated effect of Rab7 retargeting to the VROs on the late endosome and vacuole fusion events. TGE, *trans*-Golgi network; EE, early endosome; LE, late endosome; ERAS, ER arrival site subdomain in the endoplasmic reticulum.

for viral replication within VROs (34, 37, 38, 74). The above-described co-opted lipid enzymes are delivered via the hijacked retromer tubular transport carriers into VROs (37, 74).

Inhibition of retromer functions by the depletion of Rab7 or the expression of the *Legionella* DrrA effector in yeast resulted in decreased stability of the TBSV p33 or the CIRV p36 replication protein. Previously, we also observed reduced stability of the TBSV p33 and CIRV p36 replication proteins when the lipid composition of selected subcellular membranes was disturbed (18, 29, 34, 35). Therefore, it seems that usurped Rab7 and the endosomal network are critical contributors to the biogenesis of VROs with the proper lipid composition and also to the stabilization of the viral replication proteins.

Altogether, our current work reveals that Rab7 small GTPase is a major cellular target for TBSV and CIRV. We propose that tombusviruses co-opt Rab7 small GTPase to efficiently hijack the retromer complex, retromer tubular transport carriers, endosomal sorting nexin-BAR proteins, and lipid enzymes to support VRO biogenesis (Fig. 10). Rab7 might be an outstanding target for TBSV-driven subversion because the interaction between Rab7 and the Vps35 retromer component is critical for the endosomal recruitment of the retromer complex (75). Thus, usurping Rab7 might allow tombusviruses to gain access to Rab7-positive membranes, Rab7 effectors, and also the retromer complex and retromer-selected cargos.

By retargeting Rab7 into the VROs, TBSV also likely affects the other major cellular role of Rab7, which is to promote the fusion of the late endosomes (multivesicular bodies) to the lysosomes/vacuoles (76). Indeed, the interaction between Rab7 and the retromer leads to the separation of endosomal recycling from late endosome fusion with the lysosome (40). Interestingly, TBSV also recruits Rab1 and Rab5 small GTPases into VROs. Co-opting Rab1 helps TBSV to hijack the ER-derived COPII vesicles into VROs

(32). Usurping Rab5 GTPase facilitates the exploitation of the early endosomal network by TBSV (29). Overall, by hijacking several small GTPases of the Rab family, TBSV might be able to control the spatiotemporal recruitment of specific vesicular/tubular transport machineries of the host cells. Since Vps34 PI3K interacts with the yeast Rab1, Rab5, and Rab7 proteins (77), TBSV might be able to efficiently control the PI(3)P distribution in subcellular membranes by co-opting these small GTPases and Vps34p into VRCs.

Rab7 small GTPase is emerging as a major cofactor for many viruses. For example, hepatitis C virus (HCV) promotes virion secretion by modulating Rab7 activity (78). In addition, HCV also inhibits autophagy by interfering with Rab7 functions (79). The unconventional egress of severe acute respiratory syndrome coronavirus 2 (SARS-CoV-2) can be blocked by a Rab7 GTPase competitive inhibitor (80). In addition, coronavirus entry is inhibited by the loss of RAB7A, which leads to sequestering the ACE2 receptor inside cells (81). The entry and egress of several animal viruses also depend on Rab7 functions (82, 83). Hepatitis B virus is degraded by autophagy in a Rab7-dependent manner (79, 84).

In the case of plant viruses, bamboo mosaic potexvirus (BaMV) replication is affected by a plant Rab7 ortholog, whereas the cell-to-cell movement of BaMV is dependent on a Rab5 ortholog (85, 86). The cell-to-cell movement of turnip mosaic potyvirus and cauliflower mosaic virus is also affected by Rab small GTPases (87, 88). In addition to viruses, several bacterial and plant pathogens also disrupt the cellular functions of Rab7 and other Rab small GTPases to promote pathogen multiplication (58, 59, 89, 90). Prions impair lysosomal degradation by targeting Rab7 activities (91). As a regulator of autophagy, Rab7 is also a therapeutic target for neurological diseases (92).

In summary, we have discovered that tombusviruses target a major crossroad in the endocytic and recycling pathway via co-opting Rab7 small GTPase to build large VROs in infected cells. Altogether, Rab7 is co-opted by tombusviruses to produce an optimized membrane microenvironment within VROs needed for efficient tombusvirus replication. Whether other functions of Rab7 small GTPase are utilized to support TBSV replication will need additional studies.

## MATERIALS AND METHODS

**Yeast strains.** Parental yeast strain BY4741 (*MATa his3Δ1 leu2Δ0 met15Δ0 ura3Δ0*) and deletion strains *ypt7Δ*, *mon1Δ*, and *ccz1Δ* were purchased from Open Biosystems. Yeast strain BY4741::Vps34-3×HA *ypt7Δ* was created by the fusion of an HA tag to the Vps34 chromosomal location and the additional deletion of the *YPT7* gene by using yeast toolbox plasmids (93).

**Plant and yeast expression plasmids.** Plasmids pRS315-Cup1-Flag-Ypt7, pYes-p92, pEsc-p33/DI72, pYes-Strep-p95, pEsc-Strep-p36/DI72, pGD-p33-cYFP, and pEsc-GFP-p33/DI72 were described previously (29). Plasmid pRS315-Vps34-RFP was described previously (34). Plasmids pRS315-RFP-Psd2, pGD-GFP-AtPI4Kα, pRS315-RFP-Stt4, pGD-AtVps26-GFP, pGD-AtVps29-GFP, pGD-AtVps35-GFP, pRS315-RFP-Vps35, and pGD-nYFP-AtVps29 were described previously (37). Plasmids pGD-AtSnx1-GFP, pGD-AtSnx2b-GFP, pRS315-Vps5-Flag, and pGD-nYFP-AtSnx1 were described previously (38). Plasmids pGAD-Cup/FHV/ProteinA/C-Term/HA/FLAG and pESC-GAL/FHV/RNA1/Frameshift/TRSV-RZ were described previously (94).

The VIGS vector pTRV2-NbRab7(RabG3f) was constructed via PCR amplification of the NbRabG3f fragment with primer pair 8236 (CCGCTCGAGCATTGTGTGCTGGGAAAC) and 8237 (CGGGATCCAC CACAAGAGATGCAAACAATA), followed by digestion with BamHI and XhoI and insertion into BamHI- and XhoI-treated pTRV2 (95). pRS315-Flag-Ccz1 was constructed via PCR amplification of the Ccz1 fragment using primers 8356 (CGGGATCCATGAGACTACTACTATATTACGGTTTTTG) and 8357 (GCCGACGTCGAC TTAATTTCCCTGGATTCCCAC), followed by digestion with BamHI and Sall and insertion into BamHI- and Sall-treated pRS315-Flag. pGD-RFP-AtRab7B was constructed via PCR amplification of the AtRab7B fragment with primers 6538 (CGCGGATCCATGCCGTCCCGTAGACGTACC) and 6539 (ACGCGTCGACTTAGCAT TCACACCCTGTAGACCTCTGTT), followed by digestion with BamHI and Sall and insertion into BamHI- and Sall-treated pGD-RFP (96). pGD-nYFP-AtRab7B was constructed via PCR amplification of the AtRab7B fragment with primers 6538 (CGCGGATCCATGCCGTCCCGTAGACGTACC) and 6539 (ACGCGT CCGACTTAGCATTACACCCTGTAGACCTCTGTT), followed by digestion with BamHI and Sall and insertion into BamHI- and Sall-treated pGD-nYFP (29). pGD-nYFP-AtMon1 was constructed via PCR amplification of the AtMon1 fragment with primers 8448 (CGGGATCCATGGCGACTTCAGATTCTGA) and 8449 (CCGCTC GAGTACCAAGAGAAAGGACTAGC), followed by digestion with BamHI and XhoI and insertion into BamHI- and Sall-treated pGD-nYFP. pTRV2-NbMon1 was constructed via PCR amplification of the NbMon1 fragment with primers 8377 (CCGCTCGAGCACATATTTAATTTGCTTACTACAAGTTTCA) and 8378 (CGGGATCCAGGGGATCAAATGCTGCAT), followed by digestion with BamHI and XhoI and insertion into BamHI- and XhoI-treated pTRV2. pRS315-Cup1-RFP-Ypt7 was constructed via PCR amplification of

the Ypt7 fragment with primers 5783 (CGCGGATCCATGTCTTCTAGAAAAAATATTTTGAAAGTAATC) and 5784 (CCGCTCGAGTCAACAGCTACAAGAATTATTTCTCCATC), followed by digestion with BamHI and XhoI and insertion into BamHI- and SalI-treated pRS315-Cup1-RFP (29).

**Determination of viral replication in yeast and plants.** To identify the function of yeast Ypt7p small GTPase in the replication of TBSV or CIRV, yeast strains BY4741 and ypt7 $\Delta$  were transformed with plasmids pESC-His-p33/DI72, pYes-His-p92, and pRS315-Cup1-Flag or pRS315-Cup1-Flag-Ypt7 for TBSV replication or plasmids pESC-Strep-p36/DI72, pYES-Strep-p95, and pRS315-Cup1-Flag or pRS315-Cup1-Flag-Ypt7 for CIRV replication (29). The transformed yeast cells were pregrown in synthetic complete medium lacking uracil, leucine, and histidine (ULH<sup>-</sup>) supplemented with 2% glucose and 100  $\mu$ M BCS at 29°C overnight, and tombusviral repRNA replication was then launched by transferring the yeast to synthetic complete medium (ULH<sup>-</sup>) supplemented with 2% galactose and 50  $\mu$ M CuSO<sub>4</sub> at 23°C for 24 h for TBSV or 30 h for CIRV. Yeast total RNA and total protein were isolated and analyzed by Northern blotting and Western blotting, respectively (16, 27).

To investigate the role of yeast Ypt7p GEFs Mon1 and Ccz1 in TBSV replication, yeast strains BY4741, ccz1 $\Delta$ , and mon1 $\Delta$  were transformed with plasmids pEsc-His-p33/DI72, pYes-His-p92, and pRS315-Flag (29). The transformed yeast cells were pregrown in synthetic complete medium (ULH<sup>-</sup>) supplemented with 2% glucose at 29°C overnight, and tombusviral repRNA replication was then launched by transferring the yeast to synthetic complete medium (ULH<sup>-</sup>) supplemented with 2% galactose at 23°C for 24 h. Yeast total RNAs and total proteins were isolated and analyzed as described above.

To study the roles of plant Rab7 and Mon1 in tombusvirus replication, gene expression of NbRab7 or NbMon1 was downregulated with the tobacco rattle virus (TRV)-mediated virus-induced gene silencing (VIGS) system in *N. benthamiana* (95). After 12 days postagroinfiltration, the upper NbRabG3f (Rab7)- or NbMon1-silenced leaves were inoculated with TBSV or CIRV saps. The control plants were treated the same way, except using TRV-cGFP (34). Plant leaf discs from inoculated leaves were sampled for total RNA extraction and virus RNA detection. Real-time qPCR was conducted to confirm the gene knockdown by using the cDNA from upper leaves without virus inoculation (34).

**Protein colocalization assays in yeast cells.** To analyze the subcellular localization of Ypt7p in yeast cells, pYes-His-p92, pEsc-GFP-p33/DI72, and pRS315-Cup1-RFP-Ypt7 were transformed into the ypt7 $\Delta$  yeast strain. The transformed yeast cells were pregrown in synthetic complete medium (ULH<sup>-</sup>) supplemented with 2% glucose and 100  $\mu$ M BCS (bathocuproine disulphonate) at 29°C overnight. Tombusviral repRNA replication was induced by changing the medium to synthetic complete medium (ULH<sup>-</sup>) supplemented with 2% galactose and 50  $\mu$ M CuSO<sub>4</sub> for 21 h at 23°C. Yeast cells were visualized by using a 488-nm laser for GFP and a 559-nm laser for RFP in Olympus FV1200 and FV3000 confocal laser scanning microscopes.

To test the recruitment of Vps34p into viral replication compartments upon YPT7 deletion, pYes-His-p92, pEsc-GFP-p33/DI72, and pRS315-Vps34-RFP were transformed into the BY4741 and ypt7 $\Delta$  strains. Yeast cells were cultured and visualized as described above. To study the recruitment of Psd2 into viral replication compartments upon YPT7 deletion, pYes-His-p92, pEsc-GFP-p33/DI72, and pRS315-RFP-Psd2 were transformed into the BY4741 and ypt7 $\Delta$  strains. Yeast cells were cultured and visualized as described above. To test the recruitment of the yeast Stt4 into VROs upon YPT7 deletion, pYes-His-p92, pEsc-GFP-p33/DI72, and pRS315-RFP-Stt4 were transformed into the BY4741 and ypt7 $\Delta$  strains. Yeast cells were cultured and visualized as described above. To explore the co-option of retromer Vps35 into viral replication compartments upon YPT7 deletion, pYes-His-p92, pEsc-GFP-p33/DI72, and pRS315-RFP-Vps35 were transformed into the BY4741 and ypt7 $\Delta$  strains. Yeast cells were cultured and visualized as described above. To explore the co-option of sorting nexin Vps5 into viral replication compartments upon Ypt7 knockout, pYes-His-p92, pEsc-GFP-p33/DI72, and pRS315-Vps5-Flag were transformed into the BY4741 and ypt7 $\Delta$  strains. Yeast cells were cultured as described above. Immunofluorescence analysis with anti-Flag monoclonal antibody was conducted as described previously (37).

**Confocal microscopy analysis of plant cells.** To examine the subcellular localization of Rab7 in plants, *N. benthamiana* leaves were coinfiltrated with *Agrobacterium* carrying plasmids pGD-RFP-AtRab7B, pGD-GFP-SKL, or pGD-GFP-CoxIV together with pGD-p33-BFP or pGD-p36-BFP (optical density at 600 nm [OD<sub>600</sub>] of 0.3 each). The agroinfiltrated leaves were inoculated with TBSV or CIRV sap at 14 h postagroinfiltration. After 2 days postinfection (dpi), the agroinfiltrated leaves were subjected to confocal microscopy using a 405-nm laser for BFP, a 488-nm laser for GFP, and a 559-nm laser for RFP. Images were captured successively and merged using FLUOVIEW software.

To determine the interaction between Rab7 and TBSV p33 or CIRV p36 replication proteins in plants, a bimolecular fluorescence complementation (BiFC) assay was conducted in *N. benthamiana* (17). The plasmids pGD-p33-cYFP, pGD-p36-cYFP, pGD-GST-cYFP, pGD-nYFP-AtRab7B, pGD-RFP-SKL, and pGD-CoxIV-RFP were transformed into *Agrobacterium* strain C58C1 separately. The obtained *Agrobacterium* transformants were coinfiltrated (OD<sub>600</sub> of 0.3 each) into the leaves of 4-week-old *N. benthamiana* plants. Agroinfiltrated leaves were subjected to confocal laser microscopy at 60 h postagroinfiltration, followed by confocal microscopy analysis.

To determine the interaction between Mon1 and TBSV p33 replication protein in plants, a BiFC assay was conducted in *N. benthamiana*. The plasmids pGD-p33-cYFP, pGD-GST-cYFP, pGD-nYFP-AtMon1, and pGD-RFP-SKL were transformed to *Agrobacterium* strain C58C1 separately. The obtained *Agrobacterium* transformants were coinfiltrated (OD<sub>600</sub> of 0.3 each) into the leaves of 4-week-old *N. benthamiana* plants. Agroinfiltrated leaves were inoculated with TBSV sap at 14 h postagroinfiltration, and the plant samples were subjected to confocal laser microscopy 48 h after sap inoculation.

To examine the colocalization between Rab7 and PI4K upon virus infection in plants, *N. benthamiana* leaves were coinfiltrated with *Agrobacterium* carrying plasmids pGD-RFP-AtRab7B and pGD-GFP-AtPI4K $\alpha$

together with pGD-p33-BFP or pGD-p36-BFP ( $OD_{600}$  of 0.3 each). The agroinfiltrated leaves were inoculated with TBSV or CIRV sap at 14 h postagroinfiltration. After 2 dpi, the agroinfiltrated leaves were subjected to confocal microscopy as described above.

To examine the colocalization of Rab7 with retromer components upon virus infection in plants, *N. benthamiana* leaves were coinfiltrated with *Agrobacterium* carrying plasmid pGD-RFP-AtRab7B, pGD-AtVps26-GFP, or pGD-AtVps29-GFP or pGD-AtVps35-GFP together with pGD-p33-BFP ( $OD_{600}$  of 0.3 each). The agroinfiltrated leaves were inoculated with TBSV sap at 14 h postagroinfiltration. After 2 dpi, the agroinfiltrated leaves were subjected to confocal microscopy as described above.

To examine the colocalization between Rab7 and Snx1 upon virus infection in plants, *N. benthamiana* leaves were coinfiltrated with *Agrobacterium* carrying plasmids pGD-RFP-AtRab7 and pGD-AtSnx1-GFP together with pGD-p33-BFP ( $OD_{600}$  of 0.3 each). Samples were subjected to confocal microscopy as described above. To determine the recruitment of retromer Vps29 into viral replication compartments upon virus infection in RabG3f (Rab7)-silenced plants, *N. benthamiana* leaves were coinfiltrated with *Agrobacterium* carrying plasmids pGD-p33-cYFP, pGD-nYFP-AtVps29, and pGD-RFP-SKL ( $OD_{600}$  of 0.3 each). The agroinfiltrated leaves were inoculated with TBSV sap at 14 h postagroinfiltration. After 2 dpi, the agroinfiltrated leaves were subjected to confocal microscopy as described above.

To determine the recruitment of Snx1 into viral replication compartments upon virus infection in RabG3f (Rab7)-silenced plants, *N. benthamiana* leaves were coinfiltrated with *Agrobacterium* carrying plasmids pGD-p33-cYFP and pGD-nYFP-AtSnx1 together with pGD-RFP-SKL ( $OD_{600}$  of 0.1 each). The agroinfiltrated leaves were inoculated with TBSV sap at 14 h postagroinfiltration. After 2 dpi, the agroinfiltrated leaves were subjected to confocal microscopy as described above.

To determine the recruitment of Rab5 into viral replication compartments upon virus infection in RabG3f (Rab7)-silenced plants, *N. benthamiana* leaves were coinfiltrated with *Agrobacterium* carrying plasmids pGD-p33-cYFP and pGD-nYFP-AtRab5B together with pGD-RFP-SKL ( $OD_{600}$  of 0.3 each). The agroinfiltrated leaves were inoculated with TBSV sap at 14 h postagroinfiltration. After 2 dpi, the agroinfiltrated leaves were subjected to confocal microscopy as described above.

To determine the colocalization between Rab5 and Rab7 within viral replication compartments in plants, *N. benthamiana* leaves were coinfiltrated with *Agrobacterium* carrying plasmids pGD-p33-BFP and pGD-RFP-AtRab7B together with pGD-GFP-AtRab5B ( $OD_{600}$  of 0.3 each). The agroinfiltrated leaves were subjected to confocal microscopy at 48 h postagroinfiltration.

**Replicase copurification assay between p33 and Ypt7 in yeast.** To analyze the interaction between p33 and Ypt7 in yeast, pYes-His-p92, pEsc-p33/DI72, and pRS315-Cup1-Flag-Ypt7 or pRS315-Cup1-Flag were transformed into BY4741. The transformed yeast cells were pregrown in synthetic complete medium ( $ULH^-$ ) supplemented with 2% glucose and 100  $\mu$ M BCS at 29°C overnight. Tombusviral repRNA replication was induced by changing the medium to synthetic complete medium ( $ULH^-$ ) supplemented with 2% galactose and 50  $\mu$ M  $CuSO_4$  for 24 h at 23°C. Yeast cells were cross-linked by suspending yeast pellets with 1 $\times$  phosphate-buffered saline (PBS) buffer containing 1% formaldehyde for 1 h on ice. Next, glycine (to 0.1 M) was added to quench the extra formaldehyde, and the yeast cells were washed and collected by centrifugation. Yeast cells were broken with glass beads, and the membrane fraction was solubilized with 1% Triton X-100 followed by the purification of Flag-Ypt7 with anti-Flag M2 agarose (catalog number A2220; Sigma-Aldrich). The copurified protein p33 was detected by His antibody.

To analyze the interaction between p33 and Vps34 in yeast in the absence of YPT7, pGad-Cup1-Flag-p92, pGbk-Cup1-Flag-p33-Gal1-DI72, and pEsc-Ura were transformed into BY4741::Vps34-3 $\times$ HA or BY4741::Vps34-3 $\times$ HA ypt7 $\Delta$ . The transformed yeast cells were pregrown in synthetic complete medium ( $ULH^-$ ) supplemented with 2% glucose and 100  $\mu$ M BCS at 29°C overnight. This was followed by transferring the yeast cells to synthetic complete medium ( $ULH^-$ ) supplemented with 2% galactose and 100  $\mu$ M BCS at 29°C for 24 h. Tombusviral repRNA replication was induced by changing the medium to synthetic complete medium ( $ULH^-$ ) supplemented with 2% galactose and 50  $\mu$ M  $CuSO_4$  for 6 h at 23°C. A replicase copurification assay was performed as described above.

**Analyses of PE, PI(3)P, and PI(4)P enrichment within VROs in plants and yeast cells.** Plant cells and yeast cells were fixed for immunofluorescence analysis to visualize the distribution of PE, PI(3)P, and PI(4)P; detailed procedures have been described previously (19, 34, 61).

**RT-qPCR.** To monitor the gene expression of NbRabG3f and NbMon1, total RNAs were extracted from plant leaves infected with TBSV or CIRV. cDNA was synthesized for real-time qPCR analysis by using PowerUp SYBR green master mix (catalog number A25777; Thermo Fisher Scientific). Primers 8238 (CAGCAACAGTACAAGCAAC) and 8239 (GAACGCAACACCAAGACTTTG) were used for the detection of NbRabG3f (Rab7) mRNA, and primers 8379 (CTATGCGGGTGAAGAGGG) and 8380 (TGCCTTGAGAGTCGGAAAC) were used for the detection of NbMon1 mRNA levels.

**DrrA effector expression on Rab7 distribution in *N. benthamiana*.** To observe the colocalization of p33 and Rab7B in the presence or absence of the *Legionella* DrrA effector in *N. benthamiana* epidermal cells, pGD-p33-BFP, pGD-p19, pGD-GFP-SKL, pEarleyGate100-DrrA (32), and pGD-RFP-Rab7B were agroinfiltrated into *N. benthamiana* leaves, and the infiltrated leaves were inoculated with TBSV 1.5 days after agroinfiltration. The images were taken 2.5 days after infiltration.

## ACKNOWLEDGMENTS

We thank Judit Pogany for critical readings of the manuscript. We thank Kai Xu for preliminary experiments on this topic.

This work was supported by the National Science Foundation (MCB-1517751 and IOS-1922895), the USDA (NIFA, 2020-70410-32901), and a USDA hatch grant (KY012042) to P.D.N.

## REFERENCES

- Wang A. 2015. Dissecting the molecular network of virus-plant interactions: the complex roles of host factors. *Annu Rev Phytopathol* 53:45–66. <https://doi.org/10.1146/annurev-phyto-080614-120001>.
- Romero-Brey I, Bartschlagler R. 2014. Membranous replication factories induced by plus-strand RNA viruses. *Viruses* 6:2826–2857. <https://doi.org/10.3390/v6072826>.
- Nagy PD. 2016. Tombusvirus-host interactions: co-opted evolutionarily conserved host factors take center court. *Annu Rev Virol* 3:491–515. <https://doi.org/10.1146/annurev-virology-110615-042312>.
- Jordan TX, Randall G. 2016. Flavivirus modulation of cellular metabolism. *Curr Opin Virol* 19:7–10. <https://doi.org/10.1016/j.coviro.2016.05.007>.
- Shulla A, Randall G. 2016. (+) RNA virus replication compartments: a safe home for (most) viral replication. *Curr Opin Microbiol* 32:82–88. <https://doi.org/10.1016/j.mib.2016.05.003>.
- Hyodo K, Okuno T. 2020. Hijacking of host cellular components as proviral factors by plant-infecting viruses. *Adv Virus Res* 107:37–86. <https://doi.org/10.1016/bs.avir.2020.04.002>.
- Linnik O, Liesche J, Tilsner J, Oparka KJ. 2013. Unraveling the structure of viral replication complexes at super-resolution. *Front Plant Sci* 4:6. <https://doi.org/10.3389/fpls.2013.00006>.
- Laliberté JF, Zheng H. 2014. Viral manipulation of plant host membranes. *Annu Rev Virol* 1:237–259. <https://doi.org/10.1146/annurev-virology-031413-085532>.
- Kovalev N, Inaba JI, Li Z, Nagy PD. 2017. The role of co-opted ESCRT proteins and lipid factors in protection of tombusviral double-stranded RNA replication intermediate against reconstituted RNAi in yeast. *PLoS Pathog* 13:e1006520. <https://doi.org/10.1371/journal.ppat.1006520>.
- Zhang Z, He G, Filipowicz NA, Randall G, Belov GA, Kopeck BG, Wang X. 2019. Host lipids in positive-strand RNA virus genome replication. *Front Microbiol* 10:286. <https://doi.org/10.3389/fmicb.2019.00286>.
- Fernandez de Castro I, Fernandez JJ, Barajas D, Nagy PD, Risco C. 2017. Three-dimensional imaging of the intracellular assembly of a functional viral RNA replicase complex. *J Cell Sci* 130:260–268. <https://doi.org/10.1242/jcs.181586>.
- Barajas D, Martin IF, Pogany J, Risco C, Nagy PD. 2014. Noncanonical role for the host Vps4 AAA+ ATPase ESCRT protein in the formation of tomato bushy stunt virus replicase. *PLoS Pathog* 10:e1004087. <https://doi.org/10.1371/journal.ppat.1004087>.
- Nagy PD, Pogany J. 2012. The dependence of viral RNA replication on co-opted host factors. *Nat Rev Microbiol* 10:137–149. <https://doi.org/10.1038/nrmicro2692>.
- Barajas D, Jiang Y, Nagy PD. 2009. A unique role for the host ESCRT proteins in replication of Tomato bushy stunt virus. *PLoS Pathog* 5:e1000705. <https://doi.org/10.1371/journal.ppat.1000705>.
- Kovalev N, Martin IF, Pogany J, Barajas D, Pathak K, Risco C, Nagy PD. 2016. The role of viral RNA and co-opted cellular ESCRT-I and ESCRT-III factors in formation of tombusvirus spherules harboring the tombusvirus replicase. *J Virol* 90:3611–3626. <https://doi.org/10.1128/JVI.02775-15>.
- Chuang C, Prasanth KR, Nagy PD. 2017. The glycolytic pyruvate kinase is recruited directly into the viral replicase complex to generate ATP for RNA synthesis. *Cell Host Microbe* 22:639–652.e7. <https://doi.org/10.1016/j.chom.2017.10.004>.
- Barajas D, Xu K, de Castro Martin IF, Sasvari Z, Brandizzi F, Risco C, Nagy PD. 2014. Co-opted oxysterol-binding ORP and VAP proteins channel sterols to RNA virus replication sites via membrane contact sites. *PLoS Pathog* 10:e1004388. <https://doi.org/10.1371/journal.ppat.1004388>.
- Xu K, Nagy PD. 2017. Sterol binding by the tombusviral replication proteins is essential for replication in yeast and plants. *J Virol* 91:e01984-16. <https://doi.org/10.1128/JVI.01984-16>.
- Xu K, Nagy PD. 2015. RNA virus replication depends on enrichment of phosphatidylethanolamine at replication sites in subcellular membranes. *Proc Natl Acad Sci U S A* 112:E1782–E1791. <https://doi.org/10.1073/pnas.1418971112>.
- Ertel KJ, Benefield D, Castano-Diez D, Pennington JG, Horswill M, den Boon JA, Otegui MS, Ahlquist P. 2017. Cryo-electron tomography reveals novel features of a viral RNA replication compartment. *Elife* 6:e25940. <https://doi.org/10.7554/eLife.25940>.
- Paul D, Bartschlagler R. 2015. Flaviviridae replication organelles: oh, what a tangled web we weave. *Annu Rev Virol* 2:289–310. <https://doi.org/10.1146/annurev-virology-100114-055007>.
- White KA, Nagy PD. 2004. Advances in the molecular biology of tombusviruses: gene expression, genome replication, and recombination. *Prog Nucleic Acid Res Mol Biol* 78:187–226. [https://doi.org/10.1016/S0079-6603\(04\)78005-8](https://doi.org/10.1016/S0079-6603(04)78005-8).
- Stork J, Kovalev N, Sasvari Z, Nagy PD. 2011. RNA chaperone activity of the tombusviral p33 replication protein facilitates initiation of RNA synthesis by the viral RdRp in vitro. *Virology* 409:338–347. <https://doi.org/10.1016/j.virol.2010.10.015>.
- Pogany J, White KA, Nagy PD. 2005. Specific binding of tombusvirus replication protein p33 to an internal replication element in the viral RNA is essential for replication. *J Virol* 79:4859–4869. <https://doi.org/10.1128/JVI.79.8.4859-4869.2005>.
- Kovalev N, Pogany J, Nagy PD. 2020. Reconstitution of an RNA virus replicase in artificial giant unilamellar vesicles supports full replication and provides protection for the double-stranded RNA replication intermediate. *J Virol* 94:e00267-20. <https://doi.org/10.1128/JVI.00267-20>.
- Pogany J, Stork J, Li Z, Nagy PD. 2008. In vitro assembly of the Tomato bushy stunt virus replicase requires the host heat shock protein 70. *Proc Natl Acad Sci U S A* 105:19956–19961. <https://doi.org/10.1073/pnas.0810851105>.
- Panavas T, Nagy PD. 2003. Yeast as a model host to study replication and recombination of defective interfering RNA of Tomato bushy stunt virus. *Virology* 314:315–325. [https://doi.org/10.1016/s0042-6822\(03\)00436-7](https://doi.org/10.1016/s0042-6822(03)00436-7).
- Sasvari Z, Kovalev N, Gonzalez PA, Xu K, Nagy PD. 2018. Assembly-hub function of ER-localized SNARE proteins in biogenesis of tombusvirus replication compartment. *PLoS Pathog* 14:e1007028. <https://doi.org/10.1371/journal.ppat.1007028>.
- Xu K, Nagy PD. 2016. Enrichment of phosphatidylethanolamine in viral replication compartments via co-opting the endosomal Rab5 small GTPase by a positive-strand RNA virus. *PLoS Biol* 14:e2000128. <https://doi.org/10.1371/journal.pbio.2000128>.
- Pathak KB, Sasvari Z, Nagy PD. 2008. The host Pex19p plays a role in peroxisomal localization of tombusvirus replication proteins. *Virology* 379:294–305. <https://doi.org/10.1016/j.virol.2008.06.044>.
- Jonczyk M, Pathak KB, Sharma M, Nagy PD. 2007. Exploiting alternative subcellular location for replication: tombusvirus replication switches to the endoplasmic reticulum in the absence of peroxisomes. *Virology* 362:320–330. <https://doi.org/10.1016/j.virol.2007.01.004>.
- Inaba JI, Xu K, Kovalev N, Ramanathan H, Roy CR, Lindenbach BD, Nagy PD. 2019. Screening Legionella effectors for antiviral effects reveals Rab1 GTPase as a proviral factor coopted for tombusvirus replication. *Proc Natl Acad Sci U S A* 116:21739–21747. <https://doi.org/10.1073/pnas.1911108116>.
- Nagy PD, Strating JR, van Kuppeveld FJ. 2016. Building viral replication organelles: close encounters of the membrane types. *PLoS Pathog* 12:e1005912. <https://doi.org/10.1371/journal.ppat.1005912>.
- Feng Z, Xu K, Kovalev N, Nagy PD. 2019. Recruitment of Vps34 PI3K and enrichment of PI3P phosphoinositide in the viral replication compartment is crucial for replication of a positive-strand RNA virus. *PLoS Pathog* 15:e1007530. <https://doi.org/10.1371/journal.ppat.1007530>.
- Sharma M, Sasvari Z, Nagy PD. 2011. Inhibition of phospholipid biosynthesis decreases the activity of the tombusvirus replicase and alters the subcellular localization of replication proteins. *Virology* 415:141–152. <https://doi.org/10.1016/j.virol.2011.04.008>.
- Sharma M, Sasvari Z, Nagy PD. 2010. Inhibition of sterol biosynthesis reduces tombusvirus replication in yeast and plants. *J Virol* 84:2270–2281. <https://doi.org/10.1128/JVI.02003-09>.
- Feng Z, Inaba J-I, Nagy PD. 2021. The retromer is co-opted to deliver lipid enzymes for the biogenesis of lipid-enriched tombusviral replication organelles. *Proc Natl Acad Sci U S A* 118:e2016066118. <https://doi.org/10.1073/pnas.2016066118>.

38. Feng Z, Kovalev N, Nagy PD. 2020. Key interplay between the co-opted sorting nexin-BAR proteins and PI3P phosphoinositide in the formation of the tombusvirus replicase. *PLoS Pathog* 16:e1009120. <https://doi.org/10.1371/journal.ppat.1009120>.
39. Hyttinen JM, Niitykoski M, Salminen A, Kaarniranta K. 2013. Maturation of autophagosomes and endosomes: a key role for Rab7. *Biochim Biophys Acta* 1833:503–510. <https://doi.org/10.1016/j.bbamcr.2012.11.018>.
40. Purushothaman LK, Arlt H, Kuhlee A, Raunser S, Ungermann C. 2017. Retromer-driven membrane tubulation separates endosomal recycling from Rab7/Ypt7-dependent fusion. *Mol Biol Cell* 28:783–791. <https://doi.org/10.1091/mbc.E16-08-0582>.
41. Balderhaar HJ, Arlt H, Ostrowicz C, Brocker C, Sundermann F, Brandt R, Babst M, Ungermann C. 2010. The Rab GTPase Ypt7 is linked to retromer-mediated receptor recycling and fusion at the yeast late endosome. *J Cell Sci* 123:4085–4094. <https://doi.org/10.1242/jcs.071977>.
42. Stroupe C. 2018. This is the end: regulation of Rab7 nucleotide binding in endolysosomal trafficking and autophagy. *Front Cell Dev Biol* 6:129. <https://doi.org/10.3389/fcell.2018.00129>.
43. Jimenez-Organ A, Kvainickas A, Nagele H, Denner J, Eimer S, Dengjel J, Steinberg F. 2018. Control of RAB7 activity and localization through the retromer-TBC1D5 complex enables RAB7-dependent mitophagy. *EMBO J* 37:235–254. <https://doi.org/10.15252/embj.201797128>.
44. Kvainickas A, Nagele H, Qi W, Dokladal L, Jimenez-Organ A, Stehl L, Gangurde D, Zhao Q, Hu Z, Dengjel J, De Virgilio C, Baumeister R, Steinberg F. 2019. Retromer and TBC1D5 maintain late endosomal RAB7 domains to enable amino acid-induced mTORC1 signaling. *J Cell Biol* 218:3019–3038. <https://doi.org/10.1083/jcb.201812110>.
45. Guillen-Samander A, Bian X, De Camilli P. 2019. PDZD8 mediates a Rab7-dependent interaction of the ER with late endosomes and lysosomes. *Proc Natl Acad Sci U S A* 116:22619–22623. <https://doi.org/10.1073/pnas.1913509116>.
46. Wong YC, Ysselstein D, Krainc D. 2018. Mitochondria-lysosome contacts regulate mitochondrial fission via RAB7 GTP hydrolysis. *Nature* 554:382–386. <https://doi.org/10.1038/nature25486>.
47. Bouchez I, Pouteaux M, Canonge M, Genet M, Chardot T, Guillot A, Froissard M. 2015. Regulation of lipid droplet dynamics in *Saccharomyces cerevisiae* depends on the Rab7-like Ypt7p, HOPS complex and V1-ATPase. *Biol Open* 4:764–775. <https://doi.org/10.1242/bio.20148615>.
48. Guerra F, Bucci C. 2016. Multiple roles of the small GTPase Rab7. *Cells* 5:34. <https://doi.org/10.3390/cells5030034>.
49. Lucas M, Gershlick DC, Vidaurrazaga A, Rojas AL, Bonifacino JS, Hierro A. 2016. Structural mechanism for cargo recognition by the retromer complex. *Cell* 167:1623–1635.e14. <https://doi.org/10.1016/j.cell.2016.10.056>.
50. Panavas T, Serviene E, Brasher J, Nagy PD. 2005. Yeast genome-wide screen reveals dissimilar sets of host genes affecting replication of RNA viruses. *Proc Natl Acad Sci U S A* 102:7326–7331. <https://doi.org/10.1073/pnas.0502604102>.
51. Weber-Lotfi F, Dietrich A, Russo M, Rubino L. 2002. Mitochondrial targeting and membrane anchoring of a viral replicase in plant and yeast cells. *J Virol* 76:10485–10496. <https://doi.org/10.1128/jvi.76.20.10485-10496.2002>.
52. Xu K, Huang TS, Nagy PD. 2012. Authentic in vitro replication of two tombusviruses in isolated mitochondrial and endoplasmic reticulum membranes. *J Virol* 86:12779–12794. <https://doi.org/10.1128/JVI.00973-12>.
53. Cui Y, Zhao Q, Gao C, Ding Y, Zeng Y, Ueda T, Nakano A, Jiang L. 2014. Activation of the Rab7 GTPase by the MON1-CCZ1 complex is essential for PVC-to-vacuole trafficking and plant growth in *Arabidopsis*. *Plant Cell* 26:2080–2097. <https://doi.org/10.1105/tpc.114.123141>.
54. Rodriguez-Furlan C, Domozych D, Qian W, Enquist PA, Li X, Zhang C, Schenk R, Winbigler HS, Jackson W, Raikhel NV, Hicks GR. 2019. Interaction between VPS35 and RABG3f is necessary as a checkpoint to control fusion of late compartments with the vacuole. *Proc Natl Acad Sci U S A* 116:21291–21301. <https://doi.org/10.1073/pnas.1905321116>.
55. Uemura T, Ueda T. 2014. Plant vacuolar trafficking driven by RAB and SNARE proteins. *Curr Opin Plant Biol* 22:116–121. <https://doi.org/10.1016/j.pbi.2014.10.002>.
56. Dong R, Saheki Y, Swarup S, Lucast L, Harper JW, De Camilli P. 2016. Endosome-ER contacts control actin nucleation and retromer function through VAP-dependent regulation of PI4P. *Cell* 166:408–423. <https://doi.org/10.1016/j.cell.2016.06.037>.
57. Del Campo CM, Mishra AK, Wang YH, Roy CR, Janmey PA, Lambright DG. 2014. Structural basis for PI(4)P-specific membrane recruitment of the *Legionella pneumophila* effector DrrA/SidM. *Structure* 22:397–408. <https://doi.org/10.1016/j.str.2013.12.018>.
58. D'Costa VM, Braun V, Landekic M, Shi R, Proteau A, McDonald L, Cygler M, Grinstein S, Brumell JH. 2015. *Salmonella* disrupts host endocytic trafficking by SopD2-mediated inhibition of Rab7. *Cell Rep* 12:1508–1518. <https://doi.org/10.1016/j.celrep.2015.07.063>.
59. Chandra P, Ghanwat S, Matta SK, Yadav SS, Mehta M, Siddiqui Z, Singh A, Kumar D. 2015. *Mycobacterium tuberculosis* inhibits RAB7 recruitment to selectively modulate autophagy flux in macrophages. *Sci Rep* 5:16320. <https://doi.org/10.1038/srep16320>.
60. Pogany J, Nagy PD. 2015. Activation of tomato bushy stunt virus RNA-dependent RNA polymerase by cellular heat shock protein 70 is enhanced by phospholipids in vitro. *J Virol* 89:5714–5723. <https://doi.org/10.1128/JVI.03711-14>.
61. Sasvari Z, Lin W, Inaba J-I, Xu K, Kovalev N, Nagy PD. 2020. Co-opted cellular Sac1 lipid phosphatase and PI(4)P phosphoinositide are key host factors during the biogenesis of the tombusvirus replication compartment. *J Virol* 94:e01979-19. <https://doi.org/10.1128/JVI.01979-19>.
62. de Castro IF, Volonte L, Risco C. 2013. Virus factories: biogenesis and structural design. *Cell Microbiol* 15:24–34. <https://doi.org/10.1111/cmi.12029>.
63. Belov GA, van Kuppeveld FJ. 2012. (+)RNA viruses rewire cellular pathways to build replication organelles. *Curr Opin Virol* 2:740–747. <https://doi.org/10.1016/j.coviro.2012.09.006>.
64. den Boon JA, Ahlquist P. 2010. Organelle-like membrane compartmentalization of positive-strand RNA virus replication factories. *Annu Rev Microbiol* 64:241–256. <https://doi.org/10.1146/annurev.micro.112408.134012>.
65. Garcia-Ruiz H. 2018. Susceptibility genes to plant viruses. *Viruses* 10:484. <https://doi.org/10.3390/v10090484>.
66. Laliberte J-F, Sanfacon H. 2010. Cellular remodeling during plant virus infection. *Annu Rev Phytopathol* 48:69–91. <https://doi.org/10.1146/annurev-phyto-073009-114239>.
67. Reiss S, Rebhan I, Backes P, Romero-Brey I, Erfle H, Matula P, Kaderali L, Poenisch M, Blankenburg H, Hiet MS, Longrich T, Diehl S, Ramirez F, Balla T, Rohr K, Kaul A, Buhler S, Pepperkok R, Lengauer T, Albrecht M, Eils R, Schirmacher P, Lohmann V, Bartenschlager R. 2011. Recruitment and activation of a lipid kinase by hepatitis C virus NS5A is essential for integrity of the membranous replication compartment. *Cell Host Microbe* 9:32–45. <https://doi.org/10.1016/j.chom.2010.12.002>.
68. Stapleford KA, Miller DJ. 2010. Role of cellular lipids in positive-sense RNA virus replication complex assembly and function. *Viruses* 2:1055–1068. <https://doi.org/10.3390/v2051055>.
69. Xu K, Nagy PD. 2014. Expanding use of multi-origin subcellular membranes by positive-strand RNA viruses during replication. *Curr Opin Virol* 9:119–126. <https://doi.org/10.1016/j.coviro.2014.09.015>.
70. Altan-Bonnet N. 2017. Lipid tales of viral replication and transmission. *Trends Cell Biol* 27:201–213. <https://doi.org/10.1016/j.tcb.2016.09.011>.
71. van der Schaar HM, Dorobantu CM, Albuлесcu L, Strating JR, van Kuppeveld FJ. 2016. Fat(al) attraction: picornaviruses usurp lipid transfer at membrane contact sites to create replication organelles. *Trends Microbiol* 24:535–546. <https://doi.org/10.1016/j.tim.2016.02.017>.
72. Fernandez de Castro I, Tenorio R, Risco C. 2016. Virus assembly factories in a lipid world. *Curr Opin Virol* 18:20–26. <https://doi.org/10.1016/j.coviro.2016.02.009>.
73. Harak C, Lohmann V. 2015. Ultrastructure of the replication sites of positive-strand RNA viruses. *Virology* 479–480:418–433. <https://doi.org/10.1016/j.virol.2015.02.029>.
74. Nagy PD, Feng Z. 2021. Tombusviruses orchestrate the host endomembrane system to create elaborate membranous replication organelles. *Curr Opin Virol* 48:30–41. <https://doi.org/10.1016/j.coviro.2021.03.007>.
75. Priya A, Kalaidzidis IV, Kalaidzidis Y, Lambright D, Datta S. 2015. Molecular insights into Rab7-mediated endosomal recruitment of core retromer: deciphering the role of Vps26 and Vps35. *Traffic* 16:68–84. <https://doi.org/10.1111/tra.12237>.
76. Modica G, Lefrancois S. 2020. Post-translational modifications: how to modulate Rab7 functions. *Small GTPases* 11:167–173. <https://doi.org/10.1080/21541248.2017.1387686>.
77. Stein MP, Feng Y, Cooper KL, Welford AM, Wandinger-Ness A. 2003. Human VPS34 and p150 are Rab7 interacting partners. *Traffic* 4:754–771. <https://doi.org/10.1034/j.1600-0854.2003.00133.x>.
78. Wozniak AL, Long A, Jones-Jamgaard KN, Weinman SA. 2016. Hepatitis C virus promotes virion secretion through cleavage of the Rab7 adaptor protein RILP. *Proc Natl Acad Sci U S A* 113:12484–12489. <https://doi.org/10.1073/pnas.1607277113>.
79. Zhou T, Jin M, Ding Y, Zhang Y, Sun Y, Huang S, Xie Q, Xu C, Cai W. 2016. Hepatitis B virus dampens autophagy maturation via negative regulation

- of Rab7 expression. *Biosci Trends* 10:244–250. <https://doi.org/10.5582/bst.2016.01049>.
80. Ghosh S, Dellibovi-Ragheb TA, Kerviel A, Pak E, Qiu Q, Fisher M, Takvorian PM, Bleck C, Hsu VW, Fehr AR, Perlman S, Achar SR, Straus MR, Whittaker GR, de Haan CAM, Kehrl J, Altan-Bonnet G, Altan-Bonnet N. 2020.  $\beta$ -Coronaviruses use lysosomes for egress instead of the biosynthetic secretory pathway. *Cell* 183:1520–1535.e14. <https://doi.org/10.1016/j.cell.2020.10.039>.
  81. Daniloski Z, Jordan TX, Wessels H-H, Hoagland DA, Kasela S, Legut M, Maniatis S, Mimitou EP, Lu L, Geller E, Danziger O, Rosenberg BR, Phatnani H, Smibert P, Lappalainen T, tenOever BR, Sanjana NE. 2021. Identification of required host factors for SARS-CoV-2 infection in human cells. *Cell* 184:92–105.e16. <https://doi.org/10.1016/j.cell.2020.10.030>.
  82. Shi BJ, Liu CC, Zhou J, Wang SQ, Gao ZC, Zhang XM, Zhou B, Chen PY. 2016. Entry of classical swine fever virus into PK-15 cells via a pH-, dynamin-, and cholesterol-dependent, clathrin-mediated endocytic pathway that requires Rab5 and Rab7. *J Virol* 90:9194–9208. <https://doi.org/10.1128/JVI.00688-16>.
  83. Castro M, Lythe G, Smit J, Molina-París C. 2021. Fusion and fission events regulate endosome maturation and viral escape. *Sci Rep* 11:7845. <https://doi.org/10.1038/s41598-021-86877-w>.
  84. Lin Y, Wu C, Wang X, Kemper T, Squire A, Gunzer M, Zhang J, Chen X, Lu M. 2019. Hepatitis B virus is degraded by autophagosome-lysosome fusion mediated by Rab7 and related components. *Protein Cell* 10:60–66. <https://doi.org/10.1007/s13238-018-0555-2>.
  85. Huang YP, Hou PY, Chen IH, Hsu YH, Tsai CH, Cheng CP. 2020. Dissecting the role of a plant-specific Rab5 small GTPase NbRabF1 in Bamboo mosaic virus infection. *J Exp Bot* 71:6932–6944. <https://doi.org/10.1093/jxb/eraa422>.
  86. Huang YP, Jhuo JH, Tsai MS, Tsai CH, Chen HC, Lin NS, Hsu YH, Cheng CP. 2016. NbRABG3f, a member of Rab GTPase, is involved in Bamboo mosaic virus infection in *Nicotiana benthamiana*. *Mol Plant Pathol* 17:714–726. <https://doi.org/10.1111/mpp.12325>.
  87. Agbeci M, Grangeon R, Nelson RS, Zheng H, Laliberté JF. 2013. Contribution of host intracellular transport machineries to intercellular movement of turnip mosaic virus. *PLoS Pathog* 9:e1003683. <https://doi.org/10.1371/journal.ppat.1003683>.
  88. Carluccio AV, Zicca S, Stavalone L. 2014. Hitching a ride on vesicles: cauliflower mosaic virus movement protein trafficking in the endomembrane system. *Plant Physiol* 164:1261–1270. <https://doi.org/10.1104/pp.113.234534>.
  89. Lopez de Armentia MM, Gauron MC, Colombo MI. 2017. *Staphylococcus aureus* alpha-toxin induces the formation of dynamic tubules labeled with LC3 within host cells in a Rab7 and Rab1b-dependent manner. *Front Cell Infect Microbiol* 7:431. <https://doi.org/10.3389/fcimb.2017.00431>.
  90. Inada N, Betsuyaku S, Shimada TL, Ebine K, Ito E, Kutsuna N, Hasezawa S, Takano Y, Fukuda H, Nakano A, Ueda T. 2016. Modulation of plant RAB GTPase-mediated membrane trafficking pathway at the interface between plants and obligate biotrophic pathogens. *Plant Cell Physiol* 57:1854–1864. <https://doi.org/10.1093/pcp/pcw107>.
  91. Shim SY, Karri S, Law S, Schatzl HM, Gilch S. 2016. Prion infection impairs lysosomal degradation capacity by interfering with rab7 membrane attachment in neuronal cells. *Sci Rep* 6:21658. <https://doi.org/10.1038/srep21658>.
  92. Wen H, Zhan L, Chen S, Long L, Xu E. 2017. Rab7 may be a novel therapeutic target for neurologic diseases as a key regulator in autophagy. *J Neurosci Res* 95:1993–2004. <https://doi.org/10.1002/jnr.24034>.
  93. Janke C, Magiera MM, Rathfelder N, Taxis C, Reber S, Maekawa H, Moreno-Borchart A, Doenges G, Schwob E, Schiebel E, Knop M. 2004. A versatile toolbox for PCR-based tagging of yeast genes: new fluorescent proteins, more markers and promoter substitution cassettes. *Yeast* 21:947–962. <https://doi.org/10.1002/yea.1142>.
  94. Lin W, Feng Z, Prasanth KR, Liu Y, Nagy PD. 2021. Dynamic interplay between the co-opted Fis1 mitochondrial fission protein and membrane contact site proteins in supporting tombusvirus replication. *PLoS Pathog* 17:e1009423. <https://doi.org/10.1371/journal.ppat.1009423>.
  95. Dinesh-Kumar SP, Anandalakshmi R, Marathe R, Schiff M, Liu Y. 2003. Virus-induced gene silencing. *Methods Mol Biol* 236:287–294. <https://doi.org/10.1385/1-59259-413-1:287>.
  96. Goodin MM, Dietzgen RG, Schichnes D, Ruzin S, Jackson AO. 2002. pGD vectors: versatile tools for the expression of green and red fluorescent protein fusions in agroinfiltrated plant leaves. *Plant J* 31:375–383. <https://doi.org/10.1046/j.1365-313x.2002.01360.x>.